# Equivalence of on-Lattice Stochastic Chemical Kinetics with the Well-Mixed Chemical Master Equation in the Limit of Fast Diffusion

Michail Stamatakis and Dionisios G. Vlachos*
*Department of Chemical Engineering, University of Delaware, Newark, DE 19716, USA*

## ABSTRACT

Well-mixed and lattice-based descriptions of stochastic chemical kinetics have been extensively used in the literature. Realizations of the corresponding stochastic processes are obtained by the Gillespie stochastic simulation algorithm and lattice kinetic Monte Carlo algorithms, respectively. However, the two frameworks have remained disconnected. We show the equivalence of these frameworks whereby the stochastic lattice kinetics reduces to effective well-mixed kinetics in the limit of fast diffusion. In the latter, the lattice structure appears implicitly, as the lumped rate of bimolecular reactions depends on the number of neighbors of a site on the lattice. Moreover, we propose a mapping between the stochastic propensities and the deterministic rates of the well-mixed vessel and lattice dynamics that illustrates the hierarchy of models and the key parameters that enable model reduction.

**Keywords**: Master equation; time scale separation; stiffness; kinetic Monte Carlo; Gillespie algorithm; chemical kinetics

* Corresponding author. email: vlachos@udel.edu; tel. 302-831-2830.

# 1. INTRODUCTION

Stochasticity in the occurrence of chemical reactions has recently attracted significant interest in different research areas, such as biology and catalysis. In biology, the small sizes of the cellular compartments and the low numbers of molecules participating in biochemical reactions result in appreciable noise in gene expression and regulatory functions of the cell (Maheshri and O'Shea, 2007; McAdams and Arkin, 1997, 1999). This noise modulates the behavior of genetic circuits and can induce novel expression patterns, such as enhancement of cellular variability and creation or destruction of bistability (Blake et al., 2003; Hasty et al., 2000; Kepler and Elston, 2001; Raser and O'Shea, 2005; Stamatakis and Mantzaris, 2009) that have been linked to cell fate decisions (Maamar et al., 2007; Raser and O'Shea, 2005; Süel et al., 2007). In catalysis, the small sizes of systems, such as supported nanoparticle catalysts (Jacobs et al., 1997; Johánek et al., 2004; Zhdanov and Kasemo, 1998) or facets of field emitter tips (Suchorski et al., 2001; Suchorski et al., 1999), result in fluctuations in the coverages and reactivity, which have profound effects on the observed behavior. Complex phenomena, such as loss of bistability, noise-induced transitions or oscillations have been predicted by theory and confirmed by experiment (Liu and Evans, 2002; Pineda et al., 2006; Pineda et al., 2007; Vlachos et al., 1991; Zhdanov and Kasemo, 1994, 1998, 2000).

Such phenomena can be analyzed by probabilistic descriptions of chemical kinetics, which have been used for many decades to model both well-mixed and spatially-distributed systems. Well-mixed systems are described by the chemical master equation (Gardiner, 2004; McQuarrie, 1967; Nicolis and Prigogine, 1977; van Kampen, 1992), realizations of which can be obtained by an exact stochastic simulation algorithm (SSA), also known as the Gillespie kinetic Monte Carlo (KMC) algorithm (Gibson and Bruck, 2000; Gillespie, 1976, 1977). For spatially distributed systems, the lattice gas model (Kreuzer and Zhang, 1990) and the Ising spin model (Kawasaki, 1972) are used. Kinetic Monte Carlo (KMC) methods have been developed for simulating the dynamic behavior of these models (Chatterjee and Vlachos, 2007). The method is often attributed to Bortz et al. (1975).

From a theoretical standpoint, the two stochastic simulation methods, namely lattice KMC and the Gillespie SSA, remain disconnected, even though similar computational schemes are used in the simulation of lattice and well-mixed systems. Thus, in this work we are concerned with bridging the stochastic descriptions of spatially-distributed and well-mixed chemical systems. We apply singular perturbation analysis under the assumption of fast diffusion dynamics without closure assumptions or coarse-graining. We thus show that a master equation for the dynamics of a single species on the lattice reduces to a birth-death master equation that pertains to a well-mixed chemical system. This procedure elucidates the mapping between the microscopic lattice propensities and those of the well-mixed stochastic model. We further demonstrate that the error of the approximation drops linearly with the inverse of the diffusion rate. Moreover, we investigate the thermodynamic limit of large system sizes and derive deterministic models that can accurately capture the dynamics.

## 2. METHODS

Several methods have appeared in the literature for the treatment of time scale separation in chemical kinetics of well-mixed systems (Cao et al., 2005a; 2005b; E et al., 2005; Haseltine and Rawlings, 2002, 2005; Hill et al., 2008; Mastny et al., 2006, 2007; Peles et al., 2006; Rao and Arkin, 2003; Salis and Kaznessis, 2005a; 2005b; Salis et al., 2006; Samant et al., 2007; Samant and Vlachos, 2005; Weinan et al., 2007). We have extended these ideas to any type of discrete master equation by explicitly partitioning of the state space into sets within which the dynamics evolves rapidly and subsequently indexing of these sets. This procedure is essentially a coordinate transformation through which the state space is mapped to the index sets of the partition and each element of the partition. Through this mapping, conveniently chosen variables are introduced, thereby making possible the treatment of complex processes, such as the chemical kinetics of a fast diffusing species on a lattice. Previous methods can be viewed as a special case of our derivation when this mapping is linear. In the following, we summarize the key result of this derivation, the details of which appear in section 1 of the Supplementary Material along with a detailed review of previous methods.

We start from a discrete master equation of the type:

$$\frac{\partial \mathrm{P}(\mathbf{w};\mathrm{t})}{\partial \mathrm{t}} = \sum_{\mathbf{w}'\in\mathbb{W}} \left[ \alpha_{\mathbf{w}'}(\mathbf{w}) \cdot \mathrm{P}(\mathbf{w}';\mathrm{t}) - \alpha_{\mathbf{w}}(\mathbf{w}') \cdot \mathrm{P}(\mathbf{w};\mathrm{t}) \right] \tag{1}$$

where **w** and **w′** denote states belonging to $\mathbb{W}$, the state space of the system whose evolution is governed by equation (1). The latter equation is a balance for P(**w**;t), the probability that the system is in state **w** at time t. The transition probability for going from state **w′** to state **w** is denoted as $\alpha_{\mathbf{w}'}(\mathbf{w})$. Thus, the positive terms of the right hand side of equation (1) express probability influx from states **w′** to state **w**, and the negative terms express probability efflux from state **w** to state **w′**.

We subsequently introduce a partitioning in $\mathbb{W}$:

$$\begin{aligned} &\mathcal{P} = \{\mathbb{P}_{\mathbf{v}}\}_{\mathbf{v}\in\mathbb{V}} \\ &\mathbb{P}_{\mathbf{v}} \subseteq \mathbb{W} \qquad \forall\, \mathbf{v} \in \mathbb{V} \\ &\mathbb{P}_{\mathbf{v}} \cap \mathbb{P}_{\mathbf{v}'} = \varnothing \quad \forall\, \mathbf{v} \in \mathbb{V} \;\; \forall\, \mathbf{v}' \in \mathbb{V} \\ &\bigcup_{\mathbf{v}\in\mathbb{V}} \mathbb{P}_{\mathbf{v}} = \mathbb{W} \end{aligned} \tag{2}$$

This partitioning is essentially a change of coordinates which maps every state **w** to a pair of elements (**u**,**v**), where $\mathbf{v} \in \mathbb{V}$, with $\mathbb{V}$ being an index set for $\mathcal{P}$, and $\mathbf{u} \in \mathbb{U}_{\mathbf{v}}$, with $\mathbb{U}_{\mathbf{v}}$ being an index set for $\mathbb{P}_{\mathbf{v}}$. Figure 1 illustrates this mapping in a simple case where a state space consisting of 16 discrete states is partitioned to 7 disjoined sets.

If the transition probabilities of equation (1) involve large parameters that are on the order of $\varepsilon^{-1}$, $\varepsilon$ being a small parameter, one can construct a partitioning that satisfies the following condition:

$$\alpha_{\mathbf{u}',\mathbf{v}'}(\mathbf{u},\mathbf{v}) = \begin{cases} \dfrac{1}{\varepsilon}\cdot\bar{\alpha}_{\mathbf{u}',\mathbf{v}}(\mathbf{u},\mathbf{v}) & \text{if } \mathbf{v}'=\mathbf{v} \\ \bar{\alpha}_{\mathbf{u}',\mathbf{v}}(\mathbf{u},\mathbf{v}) & \text{otherwise} \end{cases} \tag{3}$$

Then, equation (1) can be decomposed to the following two equations which become exact in the limit $\varepsilon \to 0$:

$$0 = \sum_{\mathbf{u}'\in\mathbb{U}_{\mathbf{v}}} \left[\bar{\alpha}_{\mathbf{u}',\mathbf{v}}(\mathbf{u},\mathbf{v})\cdot \mathrm{P}(\mathbf{u}'\,|\,\mathbf{v};t) - \bar{\alpha}_{\mathbf{u},\mathbf{v}}(\mathbf{u}',\mathbf{v})\cdot \mathrm{P}(\mathbf{u}\,|\,\mathbf{v};t)\right] \qquad \forall\,\mathbf{v}\in\mathbb{V} \tag{4}$$

$$\begin{aligned} \frac{\partial \mathrm{P}(\mathbf{v};t)}{\partial t} = \sum_{\substack{\mathbf{v}'\in\mathbb{V}\\ \mathbf{v}'\neq\mathbf{v}}} \Bigg\{ & \left(\sum_{\mathbf{u}'\in\mathbb{U}_{\mathbf{v}'}}\sum_{\mathbf{u}\in\mathbb{U}_{\mathbf{v}}} \left[\alpha_{\mathbf{u}',\mathbf{v}'}(\mathbf{u},\mathbf{v})\cdot \mathrm{P}(\mathbf{u}'\,|\,\mathbf{v}';t)\right]\right)\cdot \mathrm{P}(\mathbf{v}';t) \\ & -\left(\sum_{\mathbf{u}'\in\mathbb{U}_{\mathbf{v}'}}\sum_{\mathbf{u}\in\mathbb{U}_{\mathbf{v}}} \left[\alpha_{\mathbf{u},\mathbf{v}}(\mathbf{u}',\mathbf{v}')\cdot \mathrm{P}(\mathbf{u}\,|\,\mathbf{v};t)\right]\right)\cdot \mathrm{P}(\mathbf{v};t)\Bigg\} \end{aligned} \tag{5}$$

Equation (4) expresses the quasi-steady-state approximation and (5) captures the slow dynamics onto which the fast ones have been projected.

# 3. THEORY

## *3.1. Model Formulation*

In this section we develop a master equation for the dynamics of adsorption, desorption, diffusion and reaction on a lattice (see Table I for the reaction network), involving a single species, and subsequently reduce this equation using the methodology of the previous section. The difference between the current work and that of Mastny et al. (2006) lies in the analytical formulation of exact and approximate mathematical models for single species lattice dynamics, whereas Mastny et al. (2006) focus on developing a numerical simulation strategy based on quasi-equilibrium arguments.

The last process appearing in Table I is the diffusional hopping of a particle to an unoccupied neighboring site, and the kinetic constant for this process is denoted as $k_{dif}$. We assume that this parameter assumes values that are much larger than any other kinetic constant. Thus, we can introduce a small parameter $\varepsilon$ and write this kinetic constant as:

$$k_{dif} = \frac{\kappa_{dif}}{\varepsilon} \tag{6}$$

where $\kappa_{dif}$ is the normalized diffusion constant, which is of the order of 1. Since $k_{dif}$ is now expressed as a parameter of order of $\varepsilon^{-1}$, it is possible to apply singular perturbation analysis.

The assumption of fast diffusion is usually valid for catalytic surfaces, for example CO diffusion is much faster than other processes on Pt surfaces (Raimondeau and Vlachos, 2002; Zhdanov and Kasemo, 1994). This, however, may not be the case when dealing with diffusion-limited processes for example those occurring in zeolites (Coppens et al., 1998; Iyengar and Coppens, 2004).

Since diffusion conserves the number of particles on a lattice, we can partition the state space into subsets in which the number of adparticles is constant (see equations 2, 3). The state of the system can then be represented as a vector of integers $(\nu,x_1,x_2,\ldots x_\nu)$, where $\nu$ denotes the number of adparticles that exist on the lattice, and $x_1,\ldots,x_\nu$ denote the sites that these particles occupy in an ascending order, so that we avoid double-counting of configurations. The corresponding master equation can be written as (see section 2 of the Supplementary Material):

$$
\begin{aligned}
\frac{\partial P(\nu, x_1, \ldots, x_\nu; t)}{\partial t} = \\
&\sum_{\xi=1}^{\nu} k_{ads} \cdot P(\nu-1, x_1, \ldots, x_{\xi-1}, x_{\xi+1}, \ldots, x_\nu; t) - \sum_{\substack{q=1,\ldots,N_L \\ q\neq x_i \forall i=1,\ldots,\nu}} k_{ads} \cdot P(\nu, x_1, \ldots, x_\nu; t) + \\
&\sum_{\substack{q=1,\ldots,N_L \\ q\neq x_i \forall i=1,\ldots,\nu}} k_{des} \cdot P(\nu+1, x_1, \ldots, q, \ldots, x_\nu; t) - \sum_{\xi=1}^{\nu} k_{des} \cdot P(\nu, x_1, \ldots x_\nu; t) + \\
&\sum_{\substack{q=1,\ldots,N_L \\ q\neq x_i \forall i=1,\ldots,\nu}} k_{rxn1} \cdot P(\nu+1, x_1, \ldots, q, \ldots, x_\nu; t) - \sum_{\xi=1}^{\nu} k_{rxn1} \cdot P(\nu, x_1, \ldots x_\nu; t) + \\
&\sum_{\substack{p=1,\ldots,N_L \\ p\neq x_i \forall i=1,\ldots,\nu}} \sum_{\substack{q=p+1,\ldots,N_L \\ q\neq x_i \forall i=1,\ldots,\nu}} k_{rxn2} \cdot \mathbf{1}_{\{p \text{ neighbors } q\}} \cdot P(\nu+2, x_1, \ldots, p, \ldots, q, \ldots, x_\nu; t) + \\
&- \sum_{\xi=1}^{\nu-1} \sum_{\varsigma=\xi+1}^{\nu} k_{rxn2} \cdot \mathbf{1}_{\{x_\xi \text{ neighbors } x_\varsigma\}} \cdot P(\nu, x_1, \ldots, x_\xi, x_\varsigma, \ldots, x_\nu; t) + \\
&\sum_{\xi=1}^{\nu} \sum_{\substack{q=1,\ldots,N_L \\ q\neq x_i \forall i=1,\ldots,\nu}} k_{dif} \cdot \mathbf{1}_{\{x_\xi \text{ neighbors } q\}} \cdot P(\nu, x_1, \ldots, x_{\xi-1}, x_{\xi+1}, \ldots, q, \ldots, x_\nu; t) + \\
&- \sum_{\xi=1}^{\nu} \sum_{\substack{q=1,\ldots,N_L \\ q\neq x_i \forall i=1,\ldots,\nu}} k_{dif} \cdot \mathbf{1}_{\{x_\xi \text{ neighbors } q\}} \cdot P(\nu, x_1, \ldots, x_\xi, \ldots, x_\nu; t)
\end{aligned}
\tag{7}
$$

Here $k_{ads}$, $k_{des}$, $k_{rxn1}$, $k_{rxn2}$, and $k_{dif}$ refer to the kinetic rates for the occurrence of each microscopic event, namely adsorption, desorption, single-site reaction, two-site reaction and diffusion, shown in Table I. Moreover, the indicator $\mathbf{1}_{\{x_i \text{ neighbors } x_j\}}$ evaluates to 1 if the two sites $x_i$ and $x_j$ are neighbors, otherwise it returns 0. State $(\nu,x_1,\ldots,x_\nu)$ may have resulted from adsorption of a particle to site $x_\xi \neq x_i$, $i = 1,\ldots,\nu$. Thus, state $(\nu,x_1,\ldots,x_\nu)$ receives probability influxes due to adsorption from all possible states containing $\nu - 1$ particles in sites $x_1,\ldots,x_{\xi-1},x_{\xi+1},\ldots,x_\nu$ (excluding site $x_\xi$). The propensity for site $x_\xi$ to become occupied in the next dt is $k_{ads}$, and $x_\xi$

may be any one of the sites $(x_1,\ldots,x_\nu)$; hence, the overall contribution of probability influxes due to adsorption events is given by the first sum of the right hand side.

Furthermore, configuration $(\nu,x_1,\ldots,x_\nu)$ has empty sites $q = 1,\ldots,N_L$ provided that $q \neq x_i$, $\forall$ $i = 1,\ldots,\nu$. Thus, adsorption to any of these sites can change the configuration, thereby generating the probability efflux term (the second sum in equation 7). The counter q over which summation is performed does not appear in the summand, since the probability is written for the occupied sites. However, q implicitly enters the calculation, in this case as a multiplication factor (the number of empty sites).

For the desorption and single site reaction processes, state $(\nu,x_1,\ldots,x_\nu)$ receives probability influx from states which have an additional adparticle at site q. The latter may take any value different from $x_1,\ldots,x_\nu$, thereby justifying the expression used in the summation over q.

The probability efflux term is justified as follows: any one of the adparticles existing in sites $x_1,\ldots,x_\nu$ can desorb giving rise to a different configuration. Thus, the probability efflux is the sum over all sites of the single site desorption terms.

For the probability influx terms due to two-site reaction events, similar arguments can be applied to derive the terms that appear in equation (7), with the only difference that we now have two additional adparticles that need to be neighboring in order to react. Thus, we sum over the possible sites that the two particles can occupy, using the indicator for sites p and q being neighbors, $\mathbf{1}_{\{p \text{ neighbors } q\}}$.

For the diffusion process, a particle jumps from site q to site $x_\xi$. Consequently, state $(\nu,x_1,\ldots,x_\nu)$ receives contributions from states in which site $x_\xi$ is unoccupied and site q is an occupied neighbor of site $x_\xi$. In a similar way, efflux terms for diffusion and reaction are calculated on the basis of the events that are allowed to happen when the system is in state $(\nu,x_1,\ldots,x_\nu)$.

### *3.2. Model Reduction*

Since diffusion does not change the number of particles on the lattice, let us introduce the marginal probability for the number of adparticles as $P(\nu;t)$ and the conditional probability for their positions $P(x_1,\ldots,x_\nu|\nu;t)$. It follows that:

$$P\left(\nu, x_1,...,x_\nu;t\right) = P\left(x_1,...,x_\nu \mid \nu;t\right)\cdot P\left(\nu;t\right) \tag{8}$$

and thus, by applying the singular perturbation methodology we reduce equation (7) to the following:

$\mathcal{O}\left(\varepsilon^{-1}\right)$:

$$P_0\left(x_1,...,x_\nu \mid \nu;t\right) = \binom{N_L}{\nu}^{-1} = \frac{\nu!\cdot\left(N_L-\nu\right)!}{N_L!} \tag{9}$$

$\mathcal{O}(1)$:

$$\frac{\partial P_0(\nu;t)}{\partial t} = k_{ads}\cdot(N_L-\nu+1)\cdot P_0(\nu-1;t) - k_{ads}\cdot(N_L-\nu)\cdot P_0(\nu;t) + k_{des}\cdot(\nu+1)\cdot P_0(\nu+1;t) - k_{des}\cdot\nu\cdot P_0(\nu;t) + k_{rxn1}\cdot(\nu+1)\cdot P_0(\nu+1;t) - k_{rxn1}\cdot\nu\cdot P_0(\nu;t) + \frac{k_{rxn2}\cdot\nu_{coord}}{2\cdot(N_L-1)}\cdot(\nu+2)\cdot(\nu+1)\cdot P_0(\nu+2;t) - \frac{k_{rxn2}\cdot\nu_{coord}}{2\cdot(N_L-1)}\cdot\nu\cdot(\nu-1)\cdot P_0(\nu;t) \quad (10)$$

where $\nu_{coord}$ is the coordination number of the lattice, namely the number of the nearest neighbors of a site. For our purposes we consider a 2D regular lattice, and thus, the coordination number can take one of the following values: 3 for a honeycomb-type lattice, 4 for a rectangular lattice, and 6 for a hexagonal lattice.

### *3.3. Deterministic Model in the Thermodynamic Limit*

By taking the limit for large system size in the birth-death master equation (10), we can formulate an ordinary differential equation (ODE) for the processes of adsorption, desorption, and reaction, which we will refer to as the thermodynamic-limit deterministic model (TL-deterministic model). Such deterministic models have been previously formulated (Mastny *et al.*, 2006). However, those were based on the chemical master equation, whereas ours are derived from the well-mixed lattice master equation (10), thereby being capable of revealing the effects of lattice connectivity and adparticle localization. Starting from equation (10) we multiply both sides with $\nu/N_L$ and sum over $\nu$:

$$\sum_{\nu=0}^{N_L}\frac{\nu}{N_L}\cdot\frac{\partial P_0(\nu;t)}{\partial t} = \sum_{\nu=1}^{N_L}k_{ads}\cdot\frac{\nu}{N_L}\cdot(N_L-\nu+1)\cdot P_0(\nu-1;t) - \sum_{\nu=0}^{N_L-1}k_{ads}\cdot\frac{\nu}{N_L}\cdot(N_L-\nu)\cdot P_0(\nu;t) + \sum_{\nu=0}^{N_L-1}k_{des}\cdot\frac{\nu}{N_L}\cdot(\nu+1)\cdot P_0(\nu+1;t) - \sum_{\nu=1}^{N_L}k_{des}\cdot\frac{\nu}{N_L}\cdot\nu\cdot P_0(\nu;t) + \sum_{\nu=0}^{N_L-1}k_{rxn1}\cdot\frac{\nu}{N_L}\cdot(\nu+1)\cdot P_0(\nu+1;t) - \sum_{\nu=1}^{N_L}k_{rxn1}\cdot\frac{\nu}{N_L}\cdot\nu\cdot P_0(\nu;t) + \sum_{\nu=0}^{N_L-2}\frac{k_{rxn2}\cdot\nu_{coord}}{2\cdot(N_L-1)}\cdot\frac{\nu}{N_L}\cdot(\nu+2)\cdot(\nu+1)\cdot P_0(\nu+2;t) - \sum_{\nu=2}^{N_L}\frac{k_{rxn2}\cdot\nu_{coord}}{2\cdot(N_L-1)}\cdot\frac{\nu}{N_L}\cdot\nu\cdot(\nu-1)\cdot P_0(\nu;t) \quad (11)$$

Subsequently, we change the summation limits of the positive terms, for instance for the 2-site reaction term:

$$\sum_{\nu=0}^{N_L-2}\frac{k_{rxn2}\cdot\nu_{coord}}{2\cdot(N_L-1)}\cdot\frac{\nu}{N_L}\cdot(\nu+2)\cdot(\nu+1)\cdot P_0(\nu+2;t) = \sum_{\nu=2}^{N_L}\frac{k_{rxn2}\cdot\nu_{coord}}{2\cdot(N_L-1)}\cdot\frac{\nu-2}{N_L}\cdot\nu\cdot(\nu-1)\cdot P_0(\nu;t) \quad (12)$$

and thus:

$$\sum_{\nu=0}^{N_L-2} \frac{k_{rxn2}\cdot\nu_{coord}}{2\cdot(N_L-1)}\cdot\frac{\nu}{N_L}\cdot(\nu+2)\cdot(\nu+1)\cdot P_0(\nu+2;t) - \sum_{\nu=2}^{N_L} \frac{k_{rxn2}\cdot\nu_{coord}}{2\cdot(N_L-1)}\cdot\frac{\nu}{N_L}\cdot\nu\cdot(\nu-1)\cdot P_0(\nu;t) = -2\cdot\frac{k_{rxn2}\cdot\nu_{coord}}{2}\cdot\sum_{\nu=2}^{N_L}\frac{\nu\cdot(\nu-1)}{N_L\cdot(N_L-1)}\cdot P_0(\nu;t) = -k_{rxn2}\cdot\nu_{coord}\cdot\left\langle\frac{\nu}{N_L}\cdot\frac{\nu-1}{N_L-1}\right\rangle \tag{13}$$

In the thermodynamic limit $N_L \to \infty$, correlations and fluctuations are suppressed:

$$\left\langle\frac{\nu}{N_L}\cdot\frac{\nu-1}{N_L-1}\right\rangle = \theta^2 \tag{14}$$

Applying the same reasoning to the rest of the terms in equation (11), one derives the following deterministic model:

$$\frac{d\theta}{dt} = r_{ads}(\theta) - r_{des}(\theta) - r_{rxn1}(\theta) - 2\cdot r_{rxn2}(\theta) \tag{15}$$

where the intensive propensity functions are given as:

$$r_{ads}(\theta) = k_{ads}\cdot(1-\theta) \tag{16}$$

$$r_{rxn1}(\theta) = k_{rxn1}\cdot\theta \tag{17}$$

$$r_{rxn2}(\theta) = \frac{k_{rxn2}}{2}\cdot\nu_{coord}\cdot\theta^2 \tag{18}$$

$$r_{des}(\theta) = k_{des}\cdot\theta \tag{19}$$

Therefore, the TL-deterministic model is written as:

$$\frac{d\theta}{dt} = k_{ads}\cdot(1-\theta) - k_{des}\cdot\theta - r_{rxn1}\cdot\theta - k_{rxn2}\cdot\nu_{coord}\cdot\theta^2 \tag{20}$$

Note that this model is identical to the mean-field models derived using the law of action kinetics (Lutsevich *et al.*, 1991). Here, equation (20) was derived using singular perturbation assuming fast Fickian diffusion and a subsequent system size expansion.

# 4. RESULTS AND DISCUSSION

## *4.1. Comparison of Microscopic Lattice KMC with Well Mixed Stochastic Kinetics*

In order to compare the full master equation (7) with the birth-death master equation (10), realizations of the corresponding stochastic processes were obtained through KMC simulations for fast diffusion dynamics. To simulate equation (7), we developed a lattice KMC code in FORTRAN 95. The code incorporates a binary tree structure for storing the partial sums of the propensities, thereby allowing for efficient $\mathcal{O}(\log_2(P))$ search and update, where P is the number of microscopic processes considered, i.e., the number of microscopic processes per site times the number of lattice sites. Note that P scales linearly with the number of lattice sites, $N_L$. On the other hand, well mixed stochastic kinetics was simulated with Gillespie's SSA algorithm, using the propensity functions appearing in equation (10). The stationary probability density was also obtained by direct solution of a system of $N_L+1$ algebraic equations, obtained by writing equation (10) at steady state for $\nu = 1,\ldots,N_L-1$, along with the following relations for $\nu = 0$ and $N_L$:

$$0 = -k_{ads}\cdot N_L\cdot P_0(0;t) + k_{des}\cdot P_0(1;t) + k_{rxn1}\cdot P_0(\nu+1;t) + \frac{k_{rxn2}\cdot\nu_{coord}}{(N_L-1)}\cdot P_0(2;t) \tag{21}$$

$$\begin{aligned} 0 = {} & k_{ads}\cdot P_0(N_L-1;t) - k_{des}\cdot N_L\cdot P_0(N_L;t) - k_{rxn1}\cdot N_L\cdot P_0(N_L;t) \\ & - \frac{k_{rxn2}\cdot\nu_{coord}}{2\cdot(N_L-1)}\cdot N_L\cdot(N_L-1)\cdot P_0(N_L;t) \end{aligned} \tag{22}$$

Figure 2 summarizes the results of these comparisons. Panel (a) shows transients of the number of adparticles on the lattice and panel (b) the corresponding stationary probability mass functions (PMFs), revealing an excellent agreement between the full and reduced model. At stationary conditions, the number of adparticles on the lattice can be viewed as a random variable that converges weakly (in distribution) to the random number of particles predicted by equation (10). The error of the approximation is on the order of $\varepsilon$ as computationally shown in panel (c). For this plot, the stationary distribution $P^s(\nu)$ was obtained though lattice KMC simulation, the approximate distribution $P_0^s(\nu)$ was obtained by solving equation (10) at steady state along with equations (21, 22) and the error was calculated as the Euclidean norm of the difference $P^s(\nu)-P_0^s(\nu)$ (see equation 13 of Supplementary Material, section 1). Furthermore, the quality of the approximation is not affected by the presence of "boundaries": excellent agreement is also observed for parameter sets for which the probability accumulates to the minimum ($\nu = 0$) or the maximum ($\nu = N_L$) number of particles as shown in Figure 2(d) and Figure 2(e).

The results obtained with the birth-death master equation (10) and the full model (7) should also agree in non-stationary conditions. To show this agreement we can solve a linear system of $N_L+1$ ordinary differential equations obtained by writing expression (10) for $\nu = 0,\ldots,N_L$ thereby computing $P_0(\nu;t)$. Subsequently, the latter can be compared to the probability distributions obtained through KMC simulations. The results of these comparisons are shown in Figure 3a, b

in which the system is initialized with an empty lattice ($P(\nu,0) = \delta_{\nu,0}$) and the two probability densities are compared at two different times. In order to perform a convergence analysis, we evaluate the two distributions at 16 time instances from 0 to $1.5 \cdot 10^{-6}$ and calculate the error as:

$$\text{Error} = \sqrt{\sum_{i=0}^{N_t} \sum_{\nu=0}^{N_L} \left( P(\nu; i \cdot \Delta t) - P_0(\nu; i \cdot \Delta t) \right)^2} \tag{23}$$

Figure 3c portrays the average $\nu$ of the birth-death equation as well as the time instances 0, $\Delta t$, $2 \cdot \Delta t$, … used in the calculation of the error (equation 23), showing that the non-stationary solution is being sampled correctly. The convergence plot of Figure 3d shows that the error drops linearly with $\varepsilon$ (see equation 6).

It is interesting to observe that the bimolecular reaction propensity that appears in equation (10) depends on the coordination number of the lattice $\nu_{coord}$, which is the number of neighbors of a site. The maximum value of $\nu_{coord}$ is $N_L - 1$ and occurs when all lattice sites are treated as neighbors. For 1$^{st}$-nearest neighbors in regular 2-dimensional lattices, the possible values of the coordination number are 3, 4 or 6 (triangular, rectangular and hexagonal lattices, respectively). Figure 4 shows the effect of lattice type on the stationary PMF for the number of adparticles. For the more connected hexagonal lattice (panels c, d), the rate of bimolecular reactions is higher, resulting in lower numbers of particles on the lattice at stationary state. If one rescales the reaction rate constant for lattices at different coordination numbers, so that the $k_{rxn2} \cdot \nu_{coord}$ is the same for these lattices, identical results are obtained (results not shown).

### *4.2. Comparison of Microscopic Lattice KMC with TL-Deterministic Model*

Figure 5 compares of the TL-deterministic model (20) with lattice KMC simulations for fast diffusion and relatively large numbers of sites. Two different lattice configurations were used, namely triangular and hexagonal lattice, in both of which the agreement between the KMC and the TL-deterministic results is excellent. Fast (Fickian) diffusion homogenizes the adsorbates on the lattice thereby rendering the approximation accurate. Our derivation and the observations just noted are in line with previously published computations comparing KMC simulation results with those obtained by ideal models employing mean-field arguments (Araya et al., 1989; Lutsevich et al., 1991; Meakin and Scalapino, 1987). For example, Lutsevich et al. (1991) observe progressively better agreement between the KMC simulations and a deterministic ideal adsorbed layer model as the coordination number of the lattice increases (maximum number of reaction partners as noted in the cited paper). Inspection of equation (20) elucidates this observation: if all sites were treated as neighbors, the coordination number would be $\nu_{coord} = N_L - 1$. For this case, the intensive reaction rate entering the mean-field model ($k_{rxn2} \cdot \nu_{coord}$) is approximately equal to the microscopic one scaled by the number of sites ($k_{rxn2} \cdot N_L$), and thus the KMC simulation and the deterministic mean-field model are in excellent agreement.

### *4.3. Computational Savings*

It is important to note that simulating the approximate models (10) or (15) is much faster than performing the full lattice KMC simulation with fast diffusion. Depending on the value of the

diffusion coefficient, the required computational time for the lattice KMC can vary from several minutes to hours. On the contrary, the corresponding simulations of the birth-death master equation typically take less than a minute and the TL-deterministic model can be simulated in a few seconds. Specifically, for fast diffusion, the computational time of the KMC increases linearly with the value of the diffusion coefficient, whereas the computational times of the approximate models remain constant. Thus, one can achieve computational speedup at least proportional to $1/\varepsilon$, namely, linear with respect $k_{dif}$ (see equation 6). This argument assumes that $\mathcal{O}(1)$ search and update algorithms are used in the lattice KMC (Chatterjee and Vlachos, 2007). In reality, the search and update algorithms are more expensive making the computational savings even larger.

### *4.4. Comparison with Chemical Master Equation and Deterministic Mass Action Law Model*

It is interesting to compare the birth-death master equation (10) and the TL-deterministic model (20) with the following chemical master equation and the corresponding deterministic model, which is based on the mass action law, respectively:

$$\begin{aligned}\frac{\partial P(\nu;t)}{\partial t} &= k_{in}^{wm}\cdot\left(N_{max}-\nu+1\right)\cdot P(\nu-1;t) - k_{in}^{wm}\cdot\left(N_{max}-\nu\right)\cdot P(\nu;t) + \\ &\quad k_{rxn1}^{wm}\cdot(\nu+1)\cdot P(\nu+1;t) - k_{rxn1}^{wm}\cdot\nu\cdot P(\nu;t) + \\ &\quad \frac{k_{rxn2}^{wm}}{2\cdot V\cdot N_A}\cdot(\nu+2)\cdot(\nu+1)\cdot P(\nu+2;t) - \frac{k_{rxn2}^{wm}}{2\cdot V\cdot N_A}\cdot\nu\cdot(\nu-1)\cdot P(\nu;t)\end{aligned} \tag{24}$$

$$\frac{dC}{dt} = k_{in}^{wm}\cdot\left(C_{max}-C\right) - k_{rxn1}^{wm}\cdot C - k_{rxn2}^{wm}\cdot C^2 \tag{25}$$

where $N_{max}$ is the maximum possible number of particles in the vessel, $C = \nu/(N_A\cdot V)$ is the concentration of particles, with $N_A$ denoting the Avogadro's number and V the volume of the vessel, and $C_{max} = N_{max}/(N_A\cdot V)$. Moreover, $k_{in}^{wm}$, $k_{rxn1}^{wm}$, and $k_{rxn2}^{wm}$ are the kinetic constants for the species inflow, and the 1st- and 2nd-order reactions, respectively (note that desorption has been omitted here for simplicity since it is a 1st-order process, in our example, like a reaction).

Furthermore, by introducing the normalized concentration:

$$\chi = \frac{C}{C_{max}} \tag{26}$$

which is analogous to the coverage fraction θ of the lattice, equation (25) becomes:

$$\frac{d\chi}{dt} = k_{in}^{wm}\cdot(1-\chi) - k_{rxn1}^{wm}\cdot\chi - k_{rxn2}^{wm}\cdot C_{max}\cdot\chi^2 \tag{27}$$

Note that the processes described by equations (24) and (25) are different from those of equations (10) and (20), since in the former, the molecules can be located anywhere in the continuous space of the vessel, whereas in the latter the molecules are localized to discrete lattice sites. Thus, the extensive reaction rates in the well-mixed vessel are affected by the volume, whereas in the lattice they are affected by the site density and neighboring structure. In the case of a vessel, bimolecular reactions occur between colliding molecules. Consequently, localization of particles in small volumes will result in more frequent collisions, and thus, higher reaction rates. For the lattice, however, bimolecular reactions occur only between neighboring molecules, and that is why the coordination number $\nu_{coord}$ appears in the 2-site reaction propensity and deterministic rate.

Despite these differences, the mathematical formalisms of equations (10, 24) and (20, 27) are analogous, thereby making possible a comparison between the two frameworks of well-mixed versus lattice-based stochastic kinetics. The differences just noted are manifested as proportionality factors in the kinetic constants found in the models. Table II reveals the mapping between the stochastic propensities and the deterministic rates of the well-mixed vessel and lattice equations. Specifically, if one wants to use a well-mixed KMC (such as the Gillespie algorithm) for capturing lattice dynamics, one would have to use the propensities appearing in the 4$^{th}$ column (Stochastic Well-Mixed Propensity) and the rows of Table II marked as "Vessel", with the following rate constants for the well-mixed case:

$$\begin{aligned} N_{max} &= N_L \\ k_{in}^{wm} &= k_{ads} \\ k_{rxn1}^{wm} &= k_{rxn1} \\ k_{rxn2}^{wm} &= k_{rxn2} \cdot \frac{\nu_{coord} \cdot V \cdot N_A}{(N_L - 1)} \end{aligned} \tag{28}$$

Similarly, simulation of a well-mixed vessel using the deterministic mass-action law equation (27) would yield identical results with the TL-deterministic model if equalities (28) hold and additionally:

$$N_L \to \infty \qquad \Rightarrow \qquad k_{rxn2}^{wm} = k_{rxn2} \cdot \frac{\nu_{coord}}{C_{max}} \tag{29}$$

## 5. CONCLUSIONS

Motivated by the challenge of bridging the stochastic descriptions of spatially distributed and well-mixed chemical systems, we studied the stochastic on-lattice kinetics of a single species and showed the equivalence of the two formulations in the fast diffusion limit.

Starting from a master equation for the processes of adsorption, desorption, diffusion and reaction of a single species on a lattice, we applied singular perturbation for fast Fickian diffusion, thereby deriving a stochastic birth-death model pertaining to a well-mixed system. This model can be simulated with the Gillespie algorithm and was found to be in excellent

agreement with the full lattice model. The quality of the approximation becomes progressively better for higher values of the diffusion coefficient and the computational savings from simulating the reduced models can be tremendous.

We further derived the deterministic model in the thermodynamic limit (TL) of large system sizes (infinite number of lattice sites). Our TL-deterministic model is identical to the Bragg-Williams mean-field formulation, when the lattice coordination number is taken into account in the kinetic constant of the two-site reaction. This reduction procedure naturally led to a mapping of the parameters of the different models in the hierarchy, thereby bridging the different levels of approximation.

## ACKNOWLEDGEMENTS

The research was partially supported by Grant Number DE-FG02-05ER25702 from the Department of Energy, NIH Grant Number P20 RR-015588 from the National Center for Research Resources, and the Center of Biomedical Research Excellence at the University of Delaware.

## REFERENCES

Araya P, Porod W, Sant R, Wolf EE. Monte-Carlo Simulations of Carbon-Monoxide Oxidation on Pt Catalysts. Surface Science 1989;208:L80-L90.

Blake WJ, Kaern M, Cantor CR, Collins JJ. Noise in eukaryotic gene expression. Nature 2003;422:633-637.

Bortz AB, Kalos MH, Lebowitz JL. New Algorithm for Monte-Carlo Simulation of Ising Spin Systems. Journal of Computational Physics 1975;17:10-18.

Cao Y, Gillespie D, Petzold L. Multiscale stochastic simulation algorithm with stochastic partial equilibrium assumption for chemically reacting systems. Journal of Computational Physics 2005a;206:395-411.

Cao Y, Gillespie DT, Petzold LR. The slow-scale stochastic simulation algorithm. Journal of Chemical Physics 2005b;122:014116.

Chatterjee A, Vlachos DG. An overview of spatial microscopic and accelerated kinetic Monte Carlo methods. Journal of Computer-Aided Materials Design 2007;14:253-308.

Coppens MO, Bell AT, Chakraborty AK. Effect of topology and molecular occupancy on self-diffusion in lattice models of zeolites - Monte-Carlo simulations. Chemical Engineering Science 1998;53:2053-2061.

E W, Liu D, Vanden-Eijnden E. Nested stochastic simulation algorithm for chemical kinetic systems with disparate rates. Journal of Chemical Physics 2005;123:194107.

Gardiner CW. Handbook of Stochastic Methods. Berlin; New York: Springer; 2004.

Gibson MA, Bruck J. Efficient Exact Stochastic Simulation of Chemical Systems with Many Species and Many Channels. The Journal of Physical Chemistry 2000;104:1876-1889.

Gillespie DT. A general method for numerically simulating the stochastic time evolution of coupled chemical reactions. Journal of Computational Physics 1976;22:403-434.

Gillespie DT. Exact stochastic simulation of coupled chemical reactions. The Journal of Physical Chemistry 1977;81:2340-2361.

Haseltine EL, Rawlings JB. Approximate simulation of coupled fast and slow reactions for stochastic chemical kinetics. The Journal of Chemical Physics 2002;117:6959-6969.
Haseltine EL, Rawlings JB. On the origins of approximations for stochastic chemical kinetics. The Journal of Chemical Physics 2005;123:164115.
Hasty J, Pradines J, Dolnik M, Collins JJ. Noise-based switches and amplifiers for gene expression. Proceedings of the National Academy of Sciences of the United States of America 2000;97:2075-2080.
Hill AD, Tomshine JR, Weeding EMB, Sotiropoulos V, Kaznessis YN. SynBioSS: the synthetic biology modeling suite. Bioinformatics 2008;24:2551-2553.
Iyengar V, Coppens MO. Dynamic Monte-Carlo simulations of binary self-diffusion in zeolites: effect of strong adsorption sites. Chemical Engineering Science 2004;59:4747-4753.
Jacobs PW, Wind SJ, Ribeiro FH, Somorjai GA. Nanometer size platinum particle arrays: Catalytic and surface chemical properties. Surface Science 1997;372:L249-L253.
Johánek V, Laurin M, Grant AW, Kasemo B, Henry CR, Libuda J. Fluctuations and bistabilities on catalyst nanoparticles. Science 2004;304:1639-1644.
Kawasaki K. In: Domb C, Green MS, editors. Phase Transitions and Critical Phenomena. New York Academic; 1972.
Kepler TB, Elston TC. Stochasticity in Transcriptional Regulation: Origins, Consequences, and Mathematical Representations. Biophysical Journal 2001;81:3116-3136.
Kreuzer HJ, Zhang J. Kinetic Lattice Gas Model: Langmuir, Ising and Interaction Kinetics. Applied Physics A-Materials Science & Processing 1990;51:183-190.
Liu DJ, Evans JW. Fluctuations and bistability in a "hybrid" atomistic model for CO oxidation on nanofacets: An effective potential analysis. Journal of Chemical Physics 2002;117:7319-7328.
Lutsevich LV, Elokhin VI, Myshlyavtsev AV, Usov AG, Yablonskii GS. Monte-Carlo Modeling of a Simple Catalytic Reaction-Mechanism - Comparison with Langmuir Kinetics. Journal of Catalysis 1991;132:302-310.
Maamar H, Raj A, Dubnau D. Noise in gene expression determines cell fate in *Bacillus subtilis*. Science 2007;317:526-529.
Maheshri N, O'Shea EK. Living with noisy genes: how cells function reliably with inherent variability in gene expression. Annual Review of Biophysics and Biomolecular Structure 2007;36:413-434.
Mastny EA, Haseltine EL, Rawlings JB. Stochastic simulation of catalytic surface reactions in the fast diffusion limit. Journal of Chemical Physics 2006;125:194715.
Mastny EA, Haseltine EL, Rawlings JB. Two classes of quasi-steady-state model reductions for stochastic kinetics. Journal of Chemical Physics 2007;127:094106.
McAdams HH, Arkin A. Stochastic mechanisms in gene expression. Proceedings of the National Academy of Sciences of the United States of America 1997;94:814-819.
McAdams HH, Arkin A. It's a noisy business! Genetic regulation at the nanomolar scale. Trends in Genetics 1999;15:65-69.
McQuarrie DA. Stochastic Approach to Chemical Kinetics. Journal of Applied Probability 1967;4:413-478.
Meakin P, Scalapino DJ. Simple-Models for Heterogeneous Catalysis - Phase Transition-Like Behavior in Nonequilibrium Systems. Journal of Chemical Physics 1987;87:731-741.
Nicolis G, Prigogine I. Self-organization in nonequilibrium systems: from dissipative structures to order through fluctuations. New York: Wiley; 1977.

Peles S, Munsky B, Khammash M. Reduction and solution of the chemical master equation using time scale separation and finite state projection. Journal of Chemical Physics 2006;125:204104.

Pineda M, Imbihl R, Schimansky-Geier L, Zulicke C. Theoretical analysis of internal fluctuations and bistability in CO oxidation on nanoscale surfaces. Journal of Chemical Physics 2006;124:044701.

Pineda M, Schimansky-Geier L, Imbihl R. Fluctuation-induced phase transition in a spatially extended model for catalytic CO oxidation. Physical Review E 2007;75:061107.

Raimondeau S, Vlachos DG. Recent developments on multiscale, hierarchical modeling of chemical reactors. Chemical Engineering Journal 2002;90:3-23.

Rao CV, Arkin AP. Stochastic chemical kinetics and the quasi-steady-state assumption: Application to the Gillespie algorithm. The Journal of Chemical Physics 2003;118:4999-5010.

Raser JM, O'Shea EK. Noise in Gene Expression: Origins, Consequences, and Control. Science 2005;309:2010-2013.

Salis H, Kaznessis Y. Accurate hybrid stochastic simulation of a system of coupled chemical or biochemical reactions. The Journal of Chemical Physics 2005a;122:054103.

Salis H, Kaznessis YN. An equation-free probabilistic steady-state approximation: Dynamic application to the stochastic simulation of biochemical reaction networks. The Journal of Chemical Physics 2005b;123:214106.

Salis H, Sotiropoulos V, Kaznessis YN. Multiscale Hy3S: Hybrid stochastic simulation for supercomputers. BMC Bioinformatics 2006;7:93.

Samant A, Ogunnaike BA, Vlachos DG. A hybrid multiscale Monte Carlo algorithm (HyMSMC) to cope with disparity in time scales and species populations in intracellular networks. BMC Bioinformatics 2007;8:175.

Samant A, Vlachos DG. Overcoming stiffness in stochastic simulation stemming from partial equilibrium: A multiscale Monte Carlo algorithm. Journal of Chemical Physics 2005;123:144114.

Stamatakis M, Mantzaris NV. Comparison of Deterministic and Stochastic Models of the lac Operon Genetic Network Biophysical Journal 2009;96:887-906.

Suchorski Y, Beben J, Imbihl R, James EW, Liu DJ, Evans JW. Fluctuations and critical phenomena in catalytic CO oxidation on nanoscale Pt facets. Physical Review B 2001;63:165417.

Suchorski Y, Beben J, James EW, Evans JW, Imbihl R. Fluctuation-induced transitions in a bistable surface reaction: Catalytic CO oxidation on a Pt field emitter tip. Physical Review Letters 1999;82:1907-1910.

Süel GM, Kulkarni RP, Dworkin J, Garcia-Ojalvo J, Elowitz MB. Tunability and noise dependence in differentiation dynamics. Science 2007;315:1716-1719.

van Kampen NG. Stochastic processes in physics and chemistry. New York, Amsterdam: North-Holland-Personal-Library; 1992.

Vlachos DG, Schmidt LD, Aris R. The Effect of Phase Transitions, Surface Diffusion, and Defects on Heterogeneous Reactions: Multiplicities and Fluctuations. Surface Science 1991;249:248-264.

Weinan E, Liu D, Vanden-Eijnden E. Nested stochastic simulation algorithms for chemical kinetic systems with multiple time scales. Journal of Computational Physics 2007;221:158-180.

Zhdanov VP, Kasemo B. Kinetic Phase-Transitions in Simple Reactions on Solid-Surfaces. Surface Science Reports 1994;20:113-189.
Zhdanov VP, Kasemo B. Monte Carlo simulation of the kinetics of rapid reactions on nanometer catalyst particles. Surface Science 1998;405:27-37.
Zhdanov VP, Kasemo B. Simulations of the reaction kinetics on nanometer supported catalyst particles. Surface Science Reports 2000;39:29-104.

# TABLES

Table I: Single Species Elementary Steps for Lattice Kinetics

| Reaction [1, 2] | Description |
|---|---|
| $*_{(s)} \xrightarrow{k_{ads}} A_{(s)}$ | Adsorption |
| $A_{(s)} \xrightarrow{k_{des}} *_{(s)}$ | 1st-order Desorption |
| $A_{(s)} \xrightarrow{k_{rxn1}} *_{(s)}$ | 1-Site, 1st-order Reaction |
| $A_{(s)} + A_{(n)} \xrightarrow{k_{rxn2}} *_{(s)} + *_{(n)}$ | 2-Site, 2nd-order Reaction |
| $A_{(s)} + *_{(n)} \xrightarrow{k_{dif}} *_{(s)} + A_{(n)}$ | Diffusion |

[1]: microscopic kinetic constants are shown.
[2]: subscripts (s) and (n) denote a site and its neighbor, respectively.

Table II: Comparison of rate expressions in various frameworks

| Process | System | Microscopic Propensity | Stochastic (Well-Mixed) Propensity | Deterministic Rate |
|---|---|---|---|---|
| Species Inflow | Lattice | $k_{ads} \cdot (1-\sigma_i)$ | $k_{ads} \cdot (N_L - \nu)$ | $k_{ads} \cdot (1-\theta)$ |
| | Vessel | – | $k_{in}^{wm} \cdot (N_{max} - \nu)$ | $k_{in}^{wm} \cdot (1-\chi)$ |
| 1st-order | Lattice | $k_{rxn1} \cdot \sigma_i$ | $k_{rxn1} \cdot \nu$ | $k_{rxn1} \cdot \theta$ |
| | Vessel | – | $k_{rxn1}^{wm} \cdot \nu$ | $k_{rxn1}^{wm} \cdot \chi$ |
| 2nd-order | Lattice | $k_{rxn2} \cdot \sigma_i \cdot \sigma_j$ | $\frac{k_{rxn2} \cdot \nu_{coord}}{2 \cdot (N_L - 1)} \cdot \nu \cdot (\nu - 1)$ | $k_{rxn2} \cdot \nu_{coord} \cdot \theta^2$ |
| | Vessel | – | $\frac{k_{rxn2}^{wm}}{2 \cdot V \cdot N_A} \cdot \nu \cdot (\nu - 1)$ | $k_{rxn2}^{wm} \cdot C_{max} \cdot \chi^2$ |

## FIGURE CAPTIONS

Figure 1: Illustration of the mapping $w \rightarrow (u,v)$. A set of 16 discrete states labeled w = 1, 2, … 16 (left schematic) can be partitioned to 7 disjoint sets $\mathbb{P}_v$, for $v \in \mathbb{V} = \{1, 2, \ldots, 7\}$ (right schematic), each of which contains a different number of states. Each of the states belonging to the same set $\mathbb{P}_v$ is assigned a "local number" u, so that the state is now specified by the ordered pair (u,v). For instance, the set $\mathbb{P}_v$ for v = 3 contains the states w = 5, 10 and 15; thus, $\mathbb{P}_3 = \{5, 10, 15\}$. The corresponding index set is $\mathbb{U}_3 = \{1, 2, 3\}$ and therefore the state w = 10 is now denoted as (u,v) = (2, 3).

Figure 2: (a): Comparison of the transients obtained with the lattice KMC and the simulation of the birth-death master equation (10). (b): Histograms corresponding to the transients of panel (a). Parameter values for panels (a, b): rectangular periodic 5 × 5 mesh ($N_L = 25$), $\nu_{coord} = 4$, $k_{ads} = 8.5\times10^5$, $k_{des} = 4.0\times10^5$, $k_{dif} = 10^9$, $k_{rxn2} = 10^6$, $t_{final} = 4\times10^{-4}$; sampling of the stochastic path was performed at time intervals $\Delta t_{sample} = 10^{-8}$. (c): The points connected with lines show the error of the approximation with respect to ε. The error was calculated as the Euclidean norm of $P^s(\nu) - P_0^s(\nu)$, in which the stationary distribution $P^s(\nu)$ is obtained through lattice KMC and the approximate one $P_0^s(\nu)$ from solving steady state equations (10-22). The straight line indicates the scaling relation C·ε where ε was evaluated as $\varepsilon = k_{ads}/k_{dif}$. (d): As in panel (b) with $k_{ads} = 8.5\times10^7$, $t_{final} = 4\times10^{-4}$. (e): As in panel (b) with $k_{ads} = 5\times10^4$, $t_{final} = 10^{-3}$.

Figure 3: (a, b): Comparison of probability distributions for the number of particles obtained with the lattice KMC and the simulation of the birth-death master equation (10) in the non-stationary regime. Multiple trajectories were run and sampled at $t = 10^{-7}$ (panel a) and $5\times10^{-7}$ (panel b). Kinetic constants as in Figure 2a. (c): The mean number of particles on the lattice as a function of time. The triangles mark the time instances used for evaluating the error in equation (23). (d): Convergence plot (similar to Figure 2c) but for the non-stationary regime. Multiple KMC trajectories were run and sampled at the times 0, $10^{-7}$, $2\times10^{-7}$, … marked in panel (c). The error was calculated from equation (23). Parameters as in panels (a, b).

Figure 4: (a): A 6 × 6 triangular lattice ($\nu_{coord} = 3$). (b): Histograms obtained from lattice and birth-death simulations of adsorption, desorption and reaction dynamics for the lattice of panel (a). Parameter values except mesh size and coordination number as in Figure 2(a). (c): A 6 × 6 hexagonal periodic lattice ($\nu_{coord} = 6$). (d): As in panel (b) for the lattice of panel (a).

Figure 5: Comparison of lattice KMC transients with mean-field results (ODE model 20). (a): Triangular periodic 30 × 30 mesh ($N_L = 900$), $\nu_{coord} = 3$. (b): Hexagonal periodic 30 × 30 mesh ($N_L = 900$), $\nu_{coord} = 6$. Other parameters: $k_{ads} = 8.5\times10^5$, $k_{des} = 4.0\times10^5$, $k_{dif} = 10^9$, $k_{rxn1} = 0$, $k_{rxn2} = 10^6$.

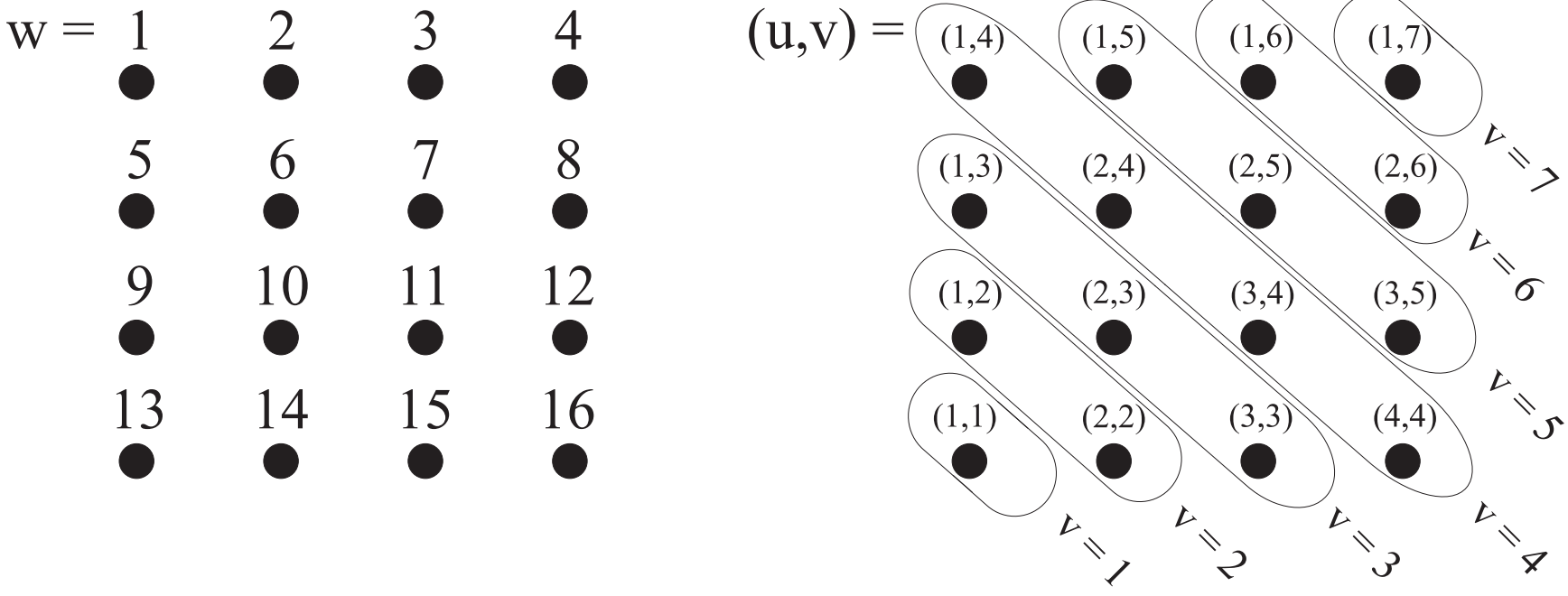
w =
1
2
3
4
5
6
7
8
9
10
11
12
13
14
15
16
(u,v) =
(1,4)
(1,5)
(1,6)
(1,7)
(1,3)
(2,4)
(2,5)
(2,6)
(1,2)
(2,3)
(3,4)
(3,5)
(1,1)
(2,2)
(3,3)
(4,4)
v=7
v=6
v=5
v=4
v=1
v=2
v=3

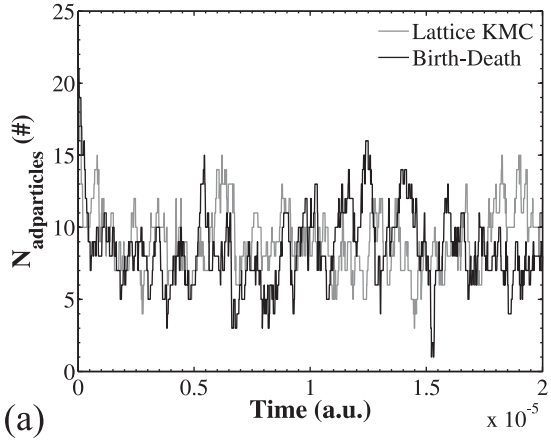
Lattice KMC
Birth-Death
$N_{adparticles}$ (#)
Time (a.u.)
x $10^{-5}$

(a)

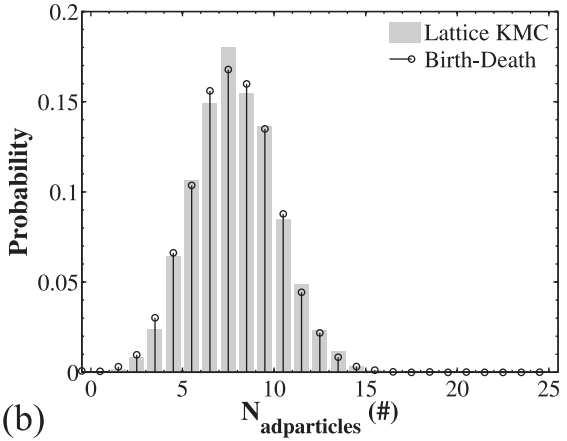
Lattice KMC
Birth-Death
Probability
$N_{adparticles}$ (#)

(b)

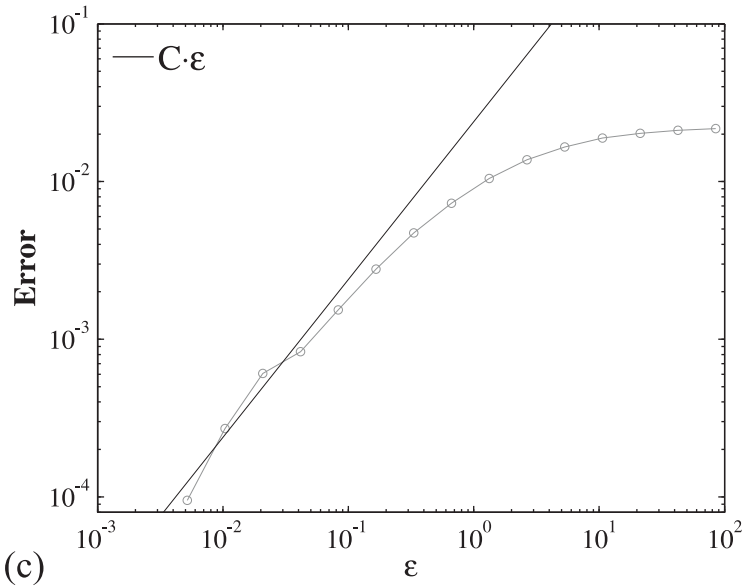
C·ε
Error
ε

(c)

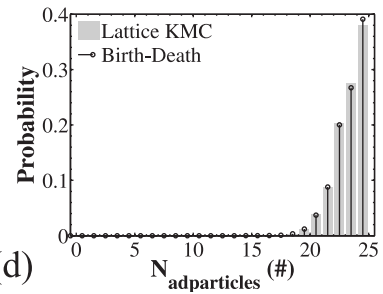
Lattice KMC
Birth-Death
Probability
$N_{adparticles}$ (#)

(d)

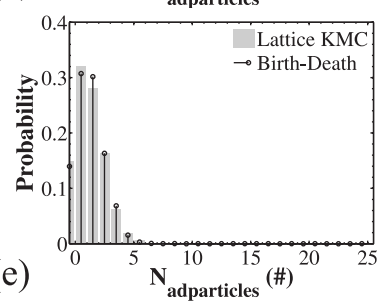
Lattice KMC
Birth-Death
Probability
$N_{adparticles}$ (#)

(e)

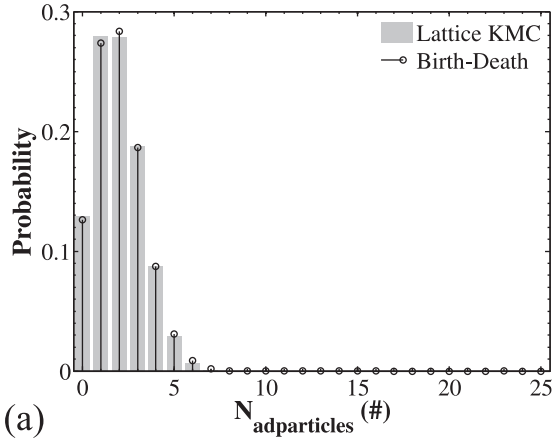
Lattice KMC
Birth-Death
Probability
0.3
0.2
0.1
0
0
5
10
15
20
25
N adparticles (#)

(a)

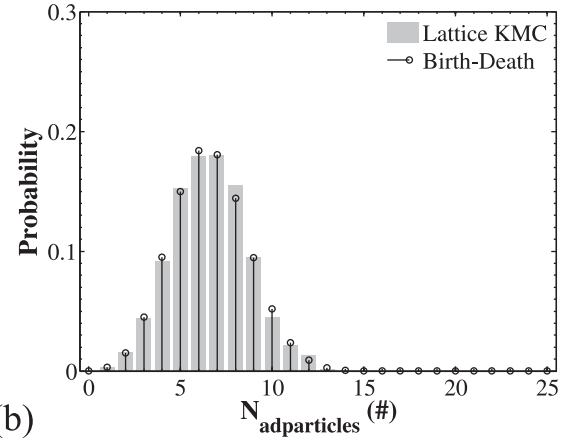
Lattice KMC
Birth-Death
Probability
0.3
0.2
0.1
0
0
5
10
15
20
25
N adparticles (#)

(b)

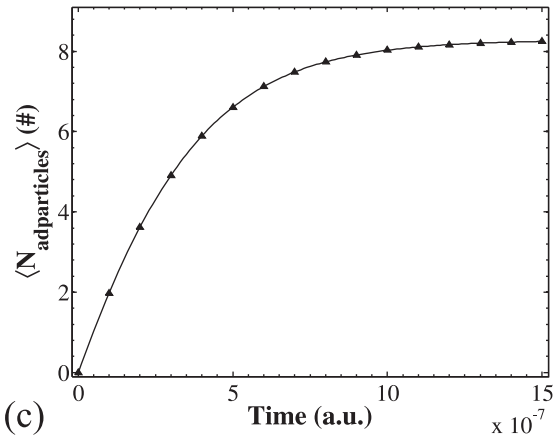
⟨N adparticles⟩ (#)
8
6
4
2
0
0
5
10
15
Time (a.u.)
x 10-7

(c)

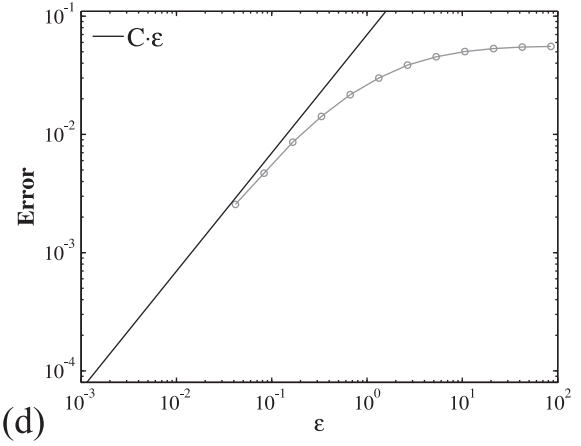
C·ε
Error
10-1
10-2
10-3
10-4
10-3
10-2
10-1
100
101
102
ε

(d)

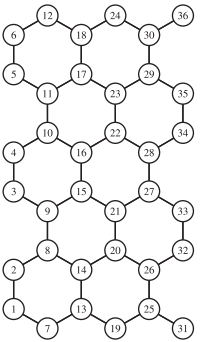
12
24
36
6
18
30
5
17
29
11
23
35
10
22
34
4
16
28
3
15
27
9
21
33
8
20
32
2
14
26
1
13
25
7
19
31

(a)

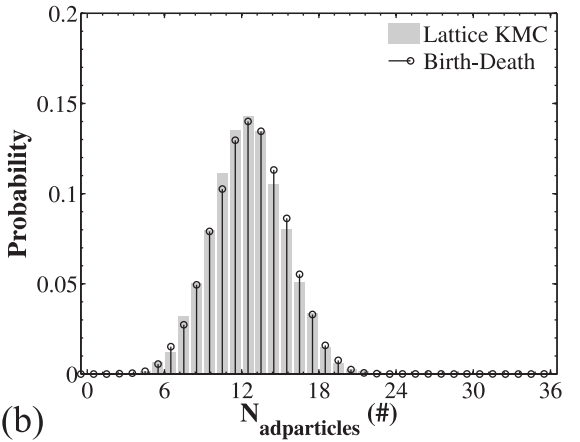
Lattice KMC
Birth-Death
Probability
0.2
0.15
0.1
0.05
0
0
6
12
18
24
30
36
N adparticles (#)

(b)

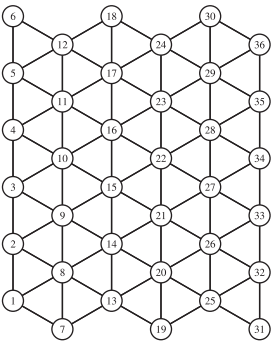
6
18
30
12
24
36
5
17
29
11
23
35
4
16
28
10
22
34
3
15
27
9
21
33
2
14
26
8
20
32
1
13
25
7
19
31

(c)

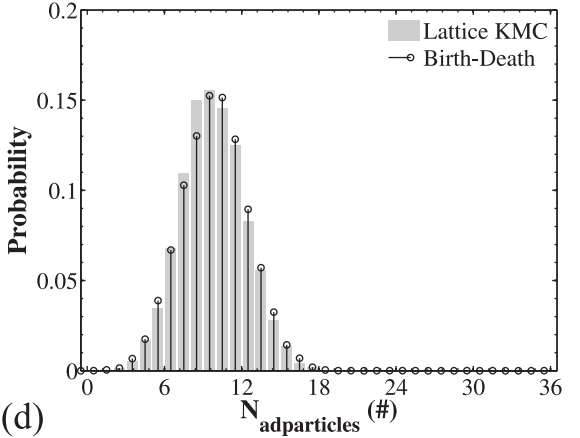
Lattice KMC
Birth-Death
Probability
0.2
0.15
0.1
0.05
0
0
6
12
18
24
30
36
N adparticles (#)

(d)

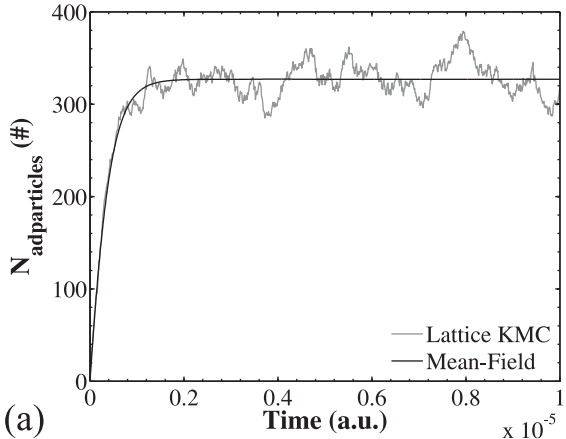
400
300
200
100
0
$N_{adparticles}$ (#)
0
0.2
0.4
0.6
0.8
1
Time (a.u.)
x $10^{-5}$
Lattice KMC
Mean-Field

(a)

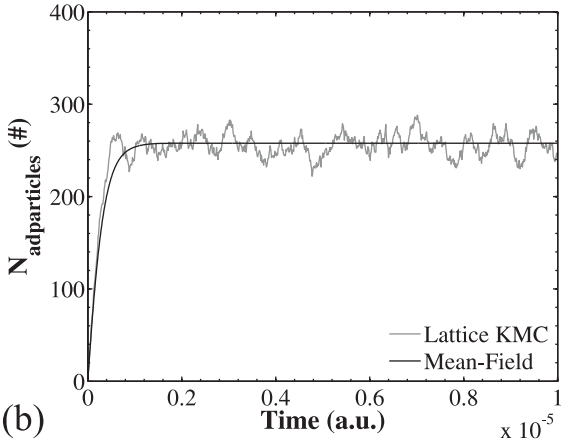
400
300
200
100
0
$N_{adparticles}$ (#)
0
0.2
0.4
0.6
0.8
1
Time (a.u.)
x $10^{-5}$
Lattice KMC
Mean-Field

(b)

# Equivalence of on-Lattice Stochastic Chemical Kinetics with the Well-Mixed Chemical Master Equation in the Limit of Fast Diffusion

Michail Stamatakis and Dionisios G. Vlachos*
*Department of Chemical Engineering, University of Delaware, Newark, DE 19716, USA*

# SUPPLEMENTARY MATERIAL

## 1. SINGULAR PERTURBATION ON DISCRETE MASTER EQUATIONS

### A. Background

The treatment of time-scale separation in the Chemical Master Equation (exact realizations of which are simulated by the Gillespie algorithm) has attracted significant attention, and several methods have been developed to this end. By partitioning the reactions into fast and slow and treat the fast ones as having reached equilibrium, hybrid and multi scale algorithms have been developed. Haseltine and Rawlings [1-2] have used such a scheme, in which Langevin formulations are used for the fast reactions and the discrete SSA [3-4] for the slow ones. In the same context, Salis and Kaznessis have proposed hybrid [5] and equation free [6] algorithms that have been integrated to freely available computational frameworks [7-8].

On the other hand, Rao and Arkin [9] partition the species into fast (ephemeral) and slow and derive a master equation for the slow species. The propensities in this equation appear as averages over the conditional probability of the fast species contents and no Langevin approximations are involved. Based on the same principle, Cao et al. [10] have developed the slow scale SSA (ssSSA) and a multiscale algorithm [11] in which the averaging of the propensities is done over the "virtual fast process", namely realizations simulating only the fast events. Samant and Vlachos [12], Samant et al. [13] and E et al. [14-15] have used singular perturbation techniques to further generalize and expand the applicability of these concepts. It is worth noting that the nested SSA [14-15] does not *a priori* define slow and fast variables, thereby allowing for linear combinations of the original variables to be used as slow observables.

Moreover, Peles et al. [16] have applied singular perturbation in conjunction with finite state projection for a class of biological problems. The latter method truncates the state space and introduces an additional error source, of which estimates can be found. A quite different approach was presented by Mastny et al. [17] who used singular perturbation for reaction networks in which the concentration of an intermediate species complex is zero. However, this method cannot be generalized to cases where the latter condition does not hold true. Finally, for the case of lattice dynamics, Mastny et al. [18] have used equilibrium assumptions (at the fast diffusion limit) to derive an approximate master equation for the number of adsorbed particles on the lattice. They demonstrated numerical results from simulating the CO oxidation on a square periodic lattice.

* Corresponding Author. e-mail: vlachos@udel.edu

## B. Methodology

Let $\mathbb{W}$ be a discrete state space and consider the master equation:

$$\frac{\partial \mathrm{P}(\mathbf{w};\mathrm{t})}{\partial \mathrm{t}} = \sum_{\mathbf{w}' \in \mathbb{W}} \left[ \alpha_{\mathbf{w}'}(\mathbf{w}) \cdot \mathrm{P}(\mathbf{w}';\mathrm{t}) - \alpha_{\mathbf{w}}(\mathbf{w}') \cdot \mathrm{P}(\mathbf{w};\mathrm{t}) \right] \tag{1}$$

In the above equation, **w** and **w′** denote states belonging to $\mathbb{W}$, the state space of the system whose evolution is governed by equation (1), P(**w**;t) is the probability that the system is in state **w** at time t, and $\alpha_{\mathbf{w}'}(\mathbf{w})$ denotes the transition probability for going from state **w′** to state **w**. Thus, the positive terms of the right hand side of equation (1) express probability influx from states **w′** to state **w**, and the negative terms express probability efflux from state **w** to state **w′**.

Let us introduce a partition in $\mathbb{W}$ as follows:

$$\begin{aligned} &\mathcal{P} = \{\mathbb{P}_{\mathbf{v}}\}_{\mathbf{v} \in \mathbb{V}} \\ &\mathbb{P}_{\mathbf{v}} \subseteq \mathbb{W} \qquad \forall\, \mathbf{v} \in \mathbb{V} \\ &\mathbb{P}_{\mathbf{v}} \cap \mathbb{P}_{\mathbf{v}'} = \varnothing \quad \forall\, \mathbf{v} \in \mathbb{V} \;\; \forall\, \mathbf{v}' \in \mathbb{V} \end{aligned} \tag{2}$$

meaning that the partition $\mathcal{P}$ is a set of disjoint subsets of $\mathbb{W}$, indexed by set $\mathbb{V}$, such that:

$$\mathbb{W} = \bigcup \mathcal{P} = \bigcup_{\mathbf{v} \in \mathbb{V}} \mathbb{P}_{\mathbf{v}} \tag{3}$$

Furthermore, each of the elements of the partition is indexed by a set $\mathbb{U}_{\mathbf{v}}$ so that:

$$\mathbb{P}_{\mathbf{v}} = \{\mathbf{w}_{\mathbf{u}}\}_{\mathbf{u} \in \mathbb{U}_{\mathbf{v}}} \tag{4}$$

Hence, the information contained in vector **w** can now be fully captured by variables $\mathbf{v} \in \mathbb{V}$ and $\mathbf{u} \in \mathbb{U}_{\mathbf{v}}$. The flow of probability in the state space $\mathbb{W}$ can be subsequently decomposed into two components: (i) intra-subset flow, namely flow between states inside the same subset $\mathbb{P}_{\mathbf{v}}$, and (ii) inter-subset flow, namely flow between states belonging to different subsets $\mathbb{P}_{\mathbf{v}}$ and $\mathbb{P}_{\mathbf{v}'}$. Let us thus introduce the probabilities and propensities in these sets:

$$\begin{aligned} &\mathrm{P}(\mathbf{w};\mathrm{t}) = \mathrm{P}(\mathbf{u},\mathbf{v};\mathrm{t}) = \mathrm{P}(\mathbf{u} \mid \mathbf{v};\mathrm{t}) \cdot \mathrm{P}(\mathbf{v};\mathrm{t}) \\ &\alpha_{\mathbf{w}}(\mathbf{w}') = \alpha_{\mathbf{u},\mathbf{v}}(\mathbf{u}',\mathbf{v}') \end{aligned} \tag{5}$$

Then, the master equation can be written as follows:

$$\frac{\partial \mathrm{P}(\mathbf{u}\,|\,\mathbf{v};\mathrm{t})\cdot \mathrm{P}(\mathbf{v};\mathrm{t})}{\partial \mathrm{t}} = \sum_{\mathbf{v}'\in\mathbb{V}} \left\{ \left( \sum_{\mathbf{u}'\in\mathbb{U}_{\mathbf{v}'}} \left[ \alpha_{\mathbf{u}',\mathbf{v}'}(\mathbf{u},\mathbf{v})\cdot \mathrm{P}(\mathbf{u}'\,|\,\mathbf{v}';\mathrm{t}) \right] \right) \cdot \mathrm{P}(\mathbf{v}';\mathrm{t}) - \left( \sum_{\mathbf{u}'\in\mathbb{U}_{\mathbf{v}'}} \left[ \alpha_{\mathbf{u},\mathbf{v}}(\mathbf{u}',\mathbf{v}')\cdot \mathrm{P}(\mathbf{u}\,|\,\mathbf{v};\mathrm{t}) \right] \right) \cdot \mathrm{P}(\mathbf{v};\mathrm{t}) \right\} \tag{6}$$

If we now apply the summing operator $\sum_{\mathbf{u}\in\mathbb{U}_{\mathbf{v}}} \bullet$ to the previous equation (6):

$$\frac{\partial \mathrm{P}(\mathbf{v};\mathrm{t})}{\partial \mathrm{t}} = \sum_{\substack{\mathbf{v}'\in\mathbb{V} \\ \mathbf{v}'\neq\mathbf{v}}} \left\{ \left( \sum_{\mathbf{u}'\in\mathbb{U}_{\mathbf{v}'}} \sum_{\mathbf{u}\in\mathbb{U}_{\mathbf{v}}} \left[ \alpha_{\mathbf{u}',\mathbf{v}'}(\mathbf{u},\mathbf{v})\cdot \mathrm{P}(\mathbf{u}'\,|\,\mathbf{v}';\mathrm{t}) \right] \right) \cdot \mathrm{P}(\mathbf{v}';\mathrm{t}) - \left( \sum_{\mathbf{u}'\in\mathbb{U}_{\mathbf{v}'}} \sum_{\mathbf{u}\in\mathbb{U}_{\mathbf{v}}} \left[ \alpha_{\mathbf{u},\mathbf{v}}(\mathbf{u}',\mathbf{v}')\cdot \mathrm{P}(\mathbf{u}\,|\,\mathbf{v};\mathrm{t}) \right] \right) \cdot \mathrm{P}(\mathbf{v};\mathrm{t}) \right\} \tag{7}$$

since the terms expressing jumps between states of the same set of the partition ($\mathbf{v} = \mathbf{v}'$) vanish:

$$\sum_{\mathbf{u}\in\mathbb{U}_{\mathbf{v}}} \sum_{\mathbf{u}'\in\mathbb{U}_{\mathbf{v}}} \left[ \alpha_{\mathbf{u}',\mathbf{v}}(\mathbf{u},\mathbf{v})\cdot \mathrm{P}(\mathbf{u}'\,|\,\mathbf{v};\mathrm{t}) - \alpha_{\mathbf{u},\mathbf{v}}(\mathbf{u}',\mathbf{v})\cdot \mathrm{P}(\mathbf{u}\,|\,\mathbf{v};\mathrm{t}) \right] = 0 \tag{8}$$

This setup makes possible the treatment of fast dynamics within subsets of $\mathbb{W}$. Specifically, assuming that the dynamics inside the subsets $\mathbb{U}_{\mathbf{v}}$ evolve fast, we can develop a master equation for the dynamics in $\mathbb{V}$. We thus consider two timescales: the probability flow inside $\mathbb{U}_{\mathbf{v}}$ occurs on the fast timescale, whereas the flow between different sets $\mathbb{U}_{\mathbf{v}}$ occurs on the slow timescale. The separation between these timescales is quantified by a single parameter ε. Thus:

$$\alpha_{\mathbf{u}',\mathbf{v}'}(\mathbf{u},\mathbf{v}) = \begin{cases} \dfrac{1}{\varepsilon}\cdot \bar{\alpha}_{\mathbf{u}',\mathbf{v}}(\mathbf{u},\mathbf{v}) & \text{if } \mathbf{v}' = \mathbf{v} \\ \bar{\alpha}_{\mathbf{u}',\mathbf{v}}(\mathbf{u},\mathbf{v}) & \text{otherwise} \end{cases} \tag{9}$$

where the value of ε depends only on the rate parameters entering the propensity functions, and $\bar{\alpha}_{\mathbf{u}',\mathbf{v}}(\mathbf{u},\mathbf{v})$ has no dependence in ε. We can subsequently introduce asymptotic expansions for the probabilities as follows:

$$\begin{aligned} \mathrm{P}(\mathbf{u}\,|\,\mathbf{v};\mathrm{t}) &= \mathrm{P}_0(\mathbf{u}\,|\,\mathbf{v};\mathrm{t}) + \varepsilon\cdot \mathrm{P}_1(\mathbf{u}\,|\,\mathbf{v};\mathrm{t}) + \varepsilon^2\cdot \mathrm{P}_2(\mathbf{u}\,|\,\mathbf{v};\mathrm{t}) + \ldots \\ \mathrm{P}(\mathbf{v};\mathrm{t}) &= \mathrm{P}_0(\mathbf{v};\mathrm{t}) + \varepsilon\cdot \mathrm{P}_1(\mathbf{v};\mathrm{t}) + \varepsilon^2\cdot \mathrm{P}_2(\mathbf{v};\mathrm{t}) + \ldots \end{aligned} \tag{10}$$

Therefore, on the order of $\varepsilon^{-1}$, equation (6) gives:

$\mathcal{O}(\varepsilon^{-1})$:

$$0 = \sum_{\mathbf{u}' \in \mathbb{U}_{\mathbf{v}}} \left[ \bar{\alpha}_{\mathbf{u}',\mathbf{v}}(\mathbf{u},\mathbf{v}) \cdot P_0(\mathbf{u}' \mid \mathbf{v};t) - \bar{\alpha}_{\mathbf{u},\mathbf{v}}(\mathbf{u}',\mathbf{v}) \cdot P_0(\mathbf{u} \mid \mathbf{v};t) \right] \qquad \forall \mathbf{v} \in \mathbb{V} \tag{11}$$

Equation (11) mathematically justifies the use of the quasi-steady-state approximation in this context. Furthermore, from equation (7) on the order of 1:

$\mathcal{O}(1)$:

$$\frac{\partial P_0(\mathbf{v};t)}{\partial t} = \sum_{\substack{\mathbf{v}' \in \mathbb{V} \\ \mathbf{v}' \neq \mathbf{v}}} \left\{ \left( \sum_{\mathbf{u}' \in \mathbb{U}_{\mathbf{v}'}} \sum_{\mathbf{u} \in \mathbb{U}_{\mathbf{v}}} \left[ \alpha_{\mathbf{u}',\mathbf{v}'}(\mathbf{u},\mathbf{v}) \cdot P_0(\mathbf{u}' \mid \mathbf{v}';t) \right] \right) \cdot P_0(\mathbf{v}';t) \right. \tag{12}$$
$$\left. - \left( \sum_{\mathbf{u}' \in \mathbb{U}_{\mathbf{v}'}} \sum_{\mathbf{u} \in \mathbb{U}_{\mathbf{v}}} \left[ \alpha_{\mathbf{u},\mathbf{v}}(\mathbf{u}',\mathbf{v}') \cdot P_0(\mathbf{u} \mid \mathbf{v};t) \right] \right) \cdot P_0(\mathbf{v};t) \right\}$$

Equation (12) has the formulation of a master equation but with propensities that are averages with respect to the posterior probability appearing in the $\mathcal{O}(\varepsilon^{-1})$ equation (11).

A few comments on the double summation are necessary to clarify the nature of this averaging. Let the system be found at pseudo-state $\mathbf{v}'$ at time t. We use the word "pseudo-state" because $\mathbf{v}$ captures only the values of the slow variables, and thus, the actual (full) state of the system is known with some uncertainty associated with the values of the fast variables $\mathbf{u}'$. Suppose now that the system transits to a pseudo-state $\mathbf{v}$. Again, there is some uncertainty as to where exactly we have landed in terms of the actual state of the system. This uncertainty exists in the values of the fast variables $\mathbf{u}$. Consequently, the double summation over $\mathbf{u}'$ and $\mathbf{u}$ essentially averages out these two sources of uncertainty: since the fast variables sample the entire partitions $\mathbb{U}_{\mathbf{v}'}$ and $\mathbb{U}_{\mathbf{v}}$, this averaging represents an averaging *from-all to-all* the possible unobserved states of the fast variables. In other words, we are averaging over all possible ways to go from $\mathbb{U}_{\mathbf{v}'}$ to $\mathbb{U}_{\mathbf{v}}$.

Note that we did not encounter any closure problems in deriving equation (12). Terms pertaining to $P_1$ no longer appear in this equation as a result of the introduction of the space partition (equation 2). We further highlight that under these conditions, the slow variables themselves follow a stochastic process that exhibits the Markov property. This is only true, of course, in the limit $\varepsilon \to 0$.

We finally note that our derivation pertains to the probabilities $P_0$ and the order of the approximation is $\varepsilon$. In the case of stationary conditions, this has the following important consequence. Suppose that the stochastic processes described by the original master equation (1) and the approximate equations (11) and (12) are both ergodic. We can thus take samples of variable $\mathbf{v}$ over time with a sampling time-lag much greater than the autocorrelation times, so that the samples are uncorrelated. Thus, we can introduce the random variables $\mathbf{v}$ and $\mathbf{v}_{\mathbf{approx}}$ pertaining to the original (1) and approximate (11, 12) master equations. The limiting behavior of $P_0$, discussed in the previous paragraph, reveals that $\mathbf{v}_{\mathbf{approx}}$ converges in distribution (weakly) to

**v**. More specifically, the error, namely the norm of the difference between the probabilities $P^s$ (satisfying the full master equation) and $P_0^s$ (satisfying the reduced model) must be 1st-order in ε:

$$\text{Error} = \sqrt{\sum_{\mathbf{v}} \left( P^s(\mathbf{v}) - P_0^s(\mathbf{v}) \right)^2} \to C \cdot \varepsilon \qquad \text{as} \qquad \varepsilon \to 0 \tag{13}$$

where C is a constant equal to the Euclidean norm of $P_1$:

$$C = \sqrt{\sum_{\mathbf{v}} \left( P_1(\mathbf{v};t) \right)^2} \tag{14}$$

## 2. LATTICE MASTER EQUATION

Consider a lattice having $N_L$ sites. The state of the system can be described with the occupancy vector **σ** whose $i^{th}$ element is 1, if site i is occupied by an adparticle, and 0 otherwise. Therefore:

$$\boldsymbol{\sigma} \in \{0,1\}^{N_L} = \mathbb{W} \tag{15}$$

Note that the state space in this case is finite containing $2^{N_L}$ elements. The Master equation describing the probability flow in the state space, dictated by the elementary steps described in Table I of the main text, is written as:

$$\begin{aligned}
&\frac{\partial P(\sigma_1,...,\sigma_{N_L})}{\partial t} = \\
&\sum_{i=1}^{N_L} k_{ads} \cdot \sigma_i \cdot P(\sigma_1,...,1-\sigma_i,...,\sigma_{N_L}) - \sum_{i=1}^{N_L} k_{ads} \cdot (1-\sigma_i) \cdot P(\sigma_1,...,\sigma_i,...,\sigma_{N_L}) + \\
&\sum_{i=1}^{N_L} k_{des} \cdot (1-\sigma_i) \cdot P(\sigma_1,...,1-\sigma_i,...,\sigma_{N_L}) - \sum_{i=1}^{N_L} k_{des} \cdot \sigma_i \cdot P(\sigma_1,...,\sigma_i,...,\sigma_{N_L}) + \\
&\sum_{i=1}^{N_L} k_{rxn1} \cdot (1-\sigma_i) \cdot P(\sigma_1,...,1-\sigma_i,...,\sigma_{N_L}) - \sum_{i=1}^{N_L} k_{rxn1} \cdot \sigma_i \cdot P(\sigma_1,...,\sigma_i,...,\sigma_{N_L}) + \\
&\sum_{i=1}^{N_L}\sum_{j=1}^{N_L} k_{rxn2} \cdot \mathbf{1}_{\{x_i \text{ neighbors } x_j\}} \cdot (1-\sigma_i) \cdot (1-\sigma_j) \cdot P(\sigma_1,...,1-\sigma_i,...,1-\sigma_j,...,\sigma_{N_L}) + \\
&\quad -\sum_{i=1}^{N_L}\sum_{j=1}^{N_L} k_{rxn2} \cdot \mathbf{1}_{\{x_i \text{ neighbors } x_j\}} \cdot \sigma_i \cdot \sigma_j \cdot P(\sigma_1,...,\sigma_i,...,\sigma_j,...,\sigma_{N_L}) + \\
&\sum_{i=1}^{N_L}\sum_{j=1}^{N_L} k_{dif} \cdot \mathbf{1}_{\{x_i \text{ neighbors } x_j\}} \cdot (1-\sigma_i) \cdot \sigma_j \cdot P(\sigma_1,...,1-\sigma_i,...,1-\sigma_j,...,\sigma_{N_L}) + \\
&\quad -\sum_{i=1}^{N_L}\sum_{j=1}^{N_L} k_{dif} \cdot \mathbf{1}_{\{x_i \text{ neighbors } x_j\}} \cdot \sigma_i \cdot (1-\sigma_j) \cdot P(\sigma_1,...,\sigma_i,...,\sigma_j,...,\sigma_{N_L})
\end{aligned} \tag{16}$$

where $k_{ads}$, $k_{des}$, $k_{rxn1}$, $k_{rxn2}$, and $k_{dif}$ refer to the kinetic rates for adsorption, desorption, single-site reaction, two-site reaction and diffusion (see Table I in main text). In the above equation, the positive terms express probability influxes from lattice configurations (states) which will result in configuration $\left(\sigma_1,...,\sigma_{N_L}\right)$ after the occurrence of a single event (adsorption, desorption, or reaction). For example, a configuration in which site i is occupied by an adparticle, ($\sigma_i = 1$ at time t), receives a probability influx due to adsorption from a configuration which had $\sigma'_i = 0$ at time t – dt. The influx term will then be written as:

$$k_{ads}\cdot\left(1-\sigma'_i\right)\cdot P\left(\sigma_1,...,\sigma'_i,...,\sigma_{N_L}\right)=k_{ads}\cdot\sigma_i\cdot P\left(\sigma_1,...,1-\sigma_i,...,\sigma_{N_L}\right)$$

Furthermore, if site i of configuration $\left(\sigma_1,...,\sigma_{N_L}\right)$ is unoccupied at time t – dt ($\sigma_i = 0$), it can accept an adparticle through adsorption, resulting in a different configuration at time t. This is expressed by the negative efflux term:

$$-k_{ads}\cdot\left(1-\sigma_i\right)\cdot P\left(\sigma_1,...,\sigma_i,...,\sigma_{N_L}\right)$$

For the desorption process, a configuration that has $\sigma'_i = 1$ at time t – dt can result in a configuration with $\sigma_i = 0$ at time t. Thus, the corresponding influx term due to desorption from site i will be:

$$k_{des}\cdot\sigma'_i\cdot P\left(\sigma_1,...,\sigma'_i,...,\sigma_{N_L}\right)=k_{des}\cdot\left(1-\sigma_i\right)\cdot P\left(\sigma_1,...,1-\sigma_i,...,\sigma_{N_L}\right)$$

Moreover, a particle existing at site i of configuration $\left(\sigma_1,...,\sigma_{N_L}\right)$ can desorb giving rise to a new configuration. This process corresponds to the following efflux term:

$$k_{des}\cdot\sigma_i\cdot P\left(\sigma_1,...,\sigma_i,...,\sigma_{N_L}\right)$$

Since the state of the lattice changes when the occupancy of any site changes, one has to sum the aforementioned terms over all lattice sites, as done in equation (16).

In the case of two-site processes, an example would be diffusion from site i to site j. The lattice configuration at time t – dt has $\sigma'_i = 1$ and $\sigma'_j = 0$ and results in configuration $\sigma_i = 0$ and $\sigma_j = 1$. Thus, the term expressing probability influx to state $\left(\sigma_1,...,\sigma_{N_L}\right)$ due to diffusion from site i to site j will be written as:

$$k_{dif}\cdot\mathbf{1}_{\{x_i \text{ neighbors } x_j\}}\cdot\sigma'_i\cdot\left(1-\sigma'_j\right)\cdot P\left(\sigma_1,...,\sigma'_i,...,\sigma'_j,...,\sigma_{N_L}\right)=$$
$$k_{dif}\cdot\mathbf{1}_{\{x_i \text{ neighbors } x_j\}}\cdot\left(1-\sigma_i\right)\cdot\sigma_j\cdot P\left(\sigma_1,...,1-\sigma_i,...,1-\sigma_j,...,\sigma_{N_L}\right)$$

By observing that diffusion does not change the number of adsorbed particles, we can partition $\mathbb{W}$ to discrete hyperplanes $\mathbb{P}_\nu$ in which the number of adsorbed particles remains constant. The collection of such hyperplanes will be indexed by the set $\mathbb{V} = \{0, 1, \ldots, N_L\}$ whose elements are the possible numbers of adsorbed particles and each hyperplane is indexed by set $\mathbb{U}_\nu$, the elements of which are vectors with the positions of the adparticles (see section 4. Lattice State Coordinate Transformation for an illustrative example). Then, by the assumption of fast diffusion, the transitions between states that belong to a hyperplane are fast and transitions between hyperplanes are slow. This allows us to apply singular perturbation analysis after introducing the following change of coordinates:

$$\boldsymbol{\sigma} \mapsto \left(\nu, x_1, ..., x_\nu\right) \tag{17}$$

where $\nu$ denotes the number of adparticles that exist on the lattice, and $x_1,\ldots,x_\nu$ denote the sites that these particles occupy in an ascending order, so that we avoid double-counting of configurations. For example, a configuration in a $3 \times 5$ lattice where sites 1, 3 and 7 are occupied will be given as:

$$\underbrace{(1,\ 0,\ 1,\ 0,\ 0,\ 0,\ 1,\ 0,\ 0,\ 0,\ 0,\ 0,\ 0,\ 0,\ 0)}_{\boldsymbol{\sigma}} \ \mapsto\ (\ \underbrace{3}_{\nu},\ \underbrace{1,\ 3,\ 7}_{x_1,\ldots,x_\nu}\ ) \tag{18}$$

Apparently:

$$\begin{aligned} &\nu \in \{0, ..., N_L\} \\ &x_i \in \{1, ..., N_L\} \ \ \forall i = 1, ..., N_L \end{aligned} \tag{19}$$

For this application we will consider adsorption, desorption, diffusional hops, as well as 1st-order and 2nd-order reactions. Let us introduce the probability of a lattice configuration $P(\nu,x_1,\ldots,x_\nu)$. The normalization condition for this probability will be written as follows:

$$P(0) + \sum_{\nu=1}^{N_L} \sum_{x_1=1}^{N_L-\nu+1} \ldots \sum_{x_\nu=1}^{N_L} P\left(\nu, x_1, ..., x_\nu; t\right) = 1 \tag{20}$$

where P(0) is the probability that no adsorbed particles exist on the lattice. The master equation that models the aforementioned processes can be written in terms of the $(\nu,x_1,\ldots,x_\nu)$ coordinates as follows (equation 12 of the main text):

$$\frac{\partial P(\nu, x_1, ..., x_\nu; t)}{\partial t} =$$

$$\sum_{\xi=1}^{\nu} k_{ads} \cdot P(\nu - 1, x_1, ..., x_{\xi-1}, x_{\xi+1}, ..., x_\nu; t) - \sum_{\substack{q=1,...,N_L \\ q \neq x_i \forall i=1,...,\nu}} k_{ads} \cdot P(\nu, x_1, ..., x_\nu; t) +$$

$$\sum_{\substack{q=1,...,N_L \\ q \neq x_i \forall i=1,...,\nu}} k_{des} \cdot P(\nu + 1, x_1, ..., q, ..., x_\nu; t) - \sum_{\xi=1}^{\nu} k_{des} \cdot P(\nu, x_1, ...x_\nu; t) +$$

$$\sum_{\substack{q=1,...,N_L \\ q \neq x_i \forall i=1,...,\nu}} k_{rxn1} \cdot P(\nu + 1, x_1, ..., q, ..., x_\nu; t) - \sum_{\xi=1}^{\nu} k_{rxn1} \cdot P(\nu, x_1, ...x_\nu; t) +$$

$$\sum_{\substack{p=1,...,N_L \\ p \neq x_i \forall i=1,...,\nu}} \sum_{\substack{q=p+1,...,N_L \\ q \neq x_i \forall i=1,...,\nu}} k_{rxn2} \cdot \mathbf{1}_{\{p \text{ neighbors } q\}} \cdot P(\nu + 2, x_1, ..., p, ..., q, ..., x_\nu; t) +$$

$$- \sum_{\xi=1}^{\nu-1} \sum_{\varsigma=\xi+1}^{\nu} k_{rxn2} \cdot \mathbf{1}_{\{x_\xi \text{ neighbors } x_\varsigma\}} \cdot P(\nu, x_1, ..., x_\xi, x_\varsigma, ..., x_\nu; t) +$$

$$\sum_{\xi=1}^{\nu} \sum_{\substack{q=1,...,N_L \\ q \neq x_i \forall i=1,...,\nu}} k_{dif} \cdot \mathbf{1}_{\{x_\xi \text{ neighbors } q\}} \cdot P(\nu, x_1, ..., x_{\xi-1}, x_{\xi+1}, ..., q, ..., x_\nu; t) +$$

$$- \sum_{\xi=1}^{\nu} \sum_{\substack{q=1,...,N_L \\ q \neq x_i \forall i=1,...,\nu}} k_{dif} \cdot \mathbf{1}_{\{x_\xi \text{ neighbors } q\}} \cdot P(\nu, x_1, ..., x_\xi, ..., x_\nu; t) \qquad (21)$$

## 3. FAST DIFFUSION APPROXIMATION

In order to apply singular perturbation according to the methodology discussed in section 1. B, we assume that $k_{dif}$, the rate constant for diffusion is large:

$$k_{dif} = \frac{\kappa_{dif}}{\varepsilon} \qquad (22)$$

where $\kappa_{dif}$ is the normalized diffusion constant, which ranges on the order of 1, and $k_{dif}$ has now been expressed as a parameter on the order of $\varepsilon^{-1}$. Since diffusion does not change the number of particles on the lattice, let us introduce the marginal probability for the number of adparticles as $P(\nu;t)$ and the conditional probability for their positions $P(x_1,\ldots,x_\nu|\nu;t)$. It follows that:

$$P(\nu, x_1, ..., x_\nu; t) = P(x_1, ..., x_\nu \mid \nu; t) \cdot P(\nu; t) \qquad (23)$$

and thus, the $\mathcal{O}(\varepsilon^{-1})$ equation is expressed as follows:

$\mathcal{O}(\varepsilon^{-1})$:

$$\sum_{\xi=1}^{\nu} \sum_{\substack{q=1,\ldots,N_L \\ q\neq x_i \forall i=1,\ldots,\nu}} \mathbf{1}_{\{x_\xi \text{ neighbors } q\}} \cdot \Big[ P_0\left(x_1,\ldots,x_{\xi-1},x_{\xi+1},\ldots,q,\ldots,x_\nu \mid \nu;t\right) - P_0\left(x_1,\ldots,x_\xi,\ldots,x_\nu \mid \nu;t\right)\Big] = 0 \tag{24}$$

which has the solution of uniform probability over the space of configurations:

$$P_0\left(x_1,\ldots,x_\nu \mid \nu;t\right) = \binom{N_L}{\nu}^{-1} = \frac{\nu!\cdot(N_L-\nu)!}{N_L!} \tag{25}$$

The $\mathcal{O}(1)$ equation for $P_0(\nu;t)$ will contain expressions of the adsorption, desorption and reaction propensities averaged with respect to the conditional probability of equation (25). Before starting to evaluate these averages, we make two observations. First, the number of terms summed in the operator:

$$\sum_{x_1=1}^{N_L-\nu+1} \cdots \sum_{x_i=x_{i-1}+1}^{N_L-\nu+i} \cdots \sum_{x_\nu=x_{\nu-1}+1}^{N_L} \bullet \tag{26}$$

is equal to the combinations of $N_L$ by $\nu$. Second, since $P(x_1,\ldots,x_\nu|\nu;t)$ is constant, averaging for one-site events essentially amounts to summing the same term multiple times. Thus, the terms for adsorption will be averaged as follows:

$$\begin{aligned} &\sum_{x_1=1}^{N_L-\nu+1} \cdots \sum_{x_i=x_{i-1}+1}^{N_L-\nu+i} \cdots \sum_{x_\nu=x_{\nu-1}+1}^{N_L} \sum_{\xi=1}^{\nu} k_{ads} \cdot P\left(x_1,\ldots,x_{\xi-1},x_{\xi+1},\ldots,x_\nu \mid \nu-1;t\right) \\ &= \binom{N_L}{\nu} \cdot \nu \cdot k_{ads} \cdot \binom{N_L}{\nu-1}^{-1} \\ &= k_{ads} \cdot (N_L-\nu+1) \end{aligned} \tag{27}$$

$$\begin{aligned} &\sum_{x_1=1}^{N_L-\nu+1} \cdots \sum_{x_i=x_{i-1}+1}^{N_L-\nu+i} \cdots \sum_{x_\nu=x_{\nu-1}+1}^{N_L} \sum_{\substack{q=1,\ldots,N_L \\ q\neq x_i \forall i=1,\ldots,\nu}} k_{ads} \cdot P\left(\nu, x_1,\ldots,x_\nu;t\right) \\ &= \binom{N_L}{\nu} \cdot (N_L-\nu) \cdot k_{ads} \cdot \binom{N_L}{\nu}^{-1} \\ &= k_{ads} \cdot (N_L-\nu) \end{aligned} \tag{28}$$

The desorption and 1st-order reaction terms are treated in the same way, therefore we only mention the former:

$$\sum_{x_1=1}^{N_L-\nu+1} \cdots \sum_{x_i=x_{i-1}+1}^{N_L-\nu+i} \cdots \sum_{x_\nu=x_{\nu-1}+1}^{N_L} \sum_{\substack{q=1 \\ q\neq x_j,\forall i=1,\ldots,\nu}}^{N_L} k_{des}\cdot P_0\left(x_1,\ldots,q,\ldots,x_\nu \mid \nu+1;t\right)$$

$$= \binom{N_L}{\nu}\cdot\left(N_L-\nu\right)\cdot k_{des}\cdot\binom{N_L}{\nu+1}^{-1} \tag{29}$$

$$= k_{des}\cdot(\nu+1)$$

$$\sum_{x_1=1}^{N_L-\nu+1} \cdots \sum_{x_i=x_{i-1}+1}^{N_L-\nu+i} \cdots \sum_{x_\nu=x_{\nu-1}+1}^{N_L} \sum_{\xi=1}^{\nu} k_{des}\cdot P_0\left(x_1,\ldots,x_\nu \mid \nu;t\right)$$

$$= \binom{N_L}{\nu}\cdot\nu\cdot k_{des}\cdot\binom{N_L}{\nu}^{-1} \tag{30}$$

$$= k_{des}\cdot\nu$$

Finally, for the treatment of 2nd-order reaction events, let us start with the efflux terms which are slightly simpler:

$$\sum_{x_1=1}^{N_L-\nu+1} \cdots \sum_{x_\nu=x_{\nu-1}+1}^{N_L} \sum_{\xi=1}^{\nu-1} \sum_{\varsigma=\xi+1}^{\nu} k_{rxn2}\cdot\mathbf{1}_{\{x_\xi \text{ neighbors } x_\varsigma\}}\cdot P_0\left(x_1,\ldots,x_\nu \mid \nu;t\right) = k_{rxn2}\cdot\left\langle N_{pairs}(\nu)\right\rangle \tag{31}$$

$\left\langle N_{pairs}(\nu)\right\rangle$ in equation (31) denotes the expected number of occupied site pairs, given that the lattice is seeded with $\nu$ adparticles, and it can be computed if we consider the expected number of occupied neighbors for an occupied site. To this end, consider the expected number of sites with j occupied neighbors, denoted as $\left\langle N^{\text{occp site}}_{\text{occp neigh,j}}(\nu)\right\rangle$. Then the expected number of pairs will be given as:

$$\left\langle N_{pairs}(\nu)\right\rangle = \frac{1}{2}\cdot\sum_{j=0}^{\nu_{coord}} j\cdot\left\langle N^{\text{occp site}}_{\text{occp neigh,j}}(\nu)\right\rangle \tag{32}$$

where the factor of ½ prevents double-counting the pairs (otherwise each pair would be counted once per occupied site and therefore two times total).

Now, we can find an analytical expression for $\left\langle N^{\text{occp site}}_{\text{occp neigh,j}}(\nu)\right\rangle$ as follows: let $\nu$ adparticles be seeded on the lattice. Given an occupied site, we want to find the probability that this site has j neighbors, where j ranges from 0 to $\nu_{coord}$, the lattice coordination number. The latter is defined as the number of nearest neighbors of a site on the lattice. The probability distribution in question is hypergeometric, since we can reformulate the problem as follows: consider a collection of the $N_L - 1$ sites, of which $N_L - \nu$ will be empty and $\nu - 1$ will be occupied. We need to sample this collection $\nu_{coord}$ times without replacement, in order to populate the neighbors of the given occupied site. We then ask what is the probability that j out of the $\nu_{coord}$

sites will be occupied. Clearly, the number of successes will follow a hypergeometric distribution, and thus:

$$\frac{\left\langle N^{\text{occp site}}_{\text{occp neigh},j}(\nu)\right\rangle}{\nu} = \binom{N_L-\nu}{\nu_{\text{coord}}-j}\cdot\binom{\nu-1}{j}\cdot\binom{N_L-1}{\nu_{\text{coord}}}^{-1} \tag{33}$$

and therefore:

$$\left\langle N_{\text{pairs}}(\nu)\right\rangle = \frac{1}{2}\cdot\nu\cdot\sum_{j=0}^{\nu_{\text{coord}}} j\cdot\binom{N_L-\nu}{\nu_{\text{coord}}-j}\cdot\binom{\nu-1}{j}\cdot\binom{N_L-1}{\nu_{\text{coord}}}^{-1} \tag{34}$$

The sum evaluates to the average of the hypergeometric distribution, which is equal to the product of total number of samplings and maximum number of successes divided by the size of the sampled population. Therefore, in our case:

$$\left\langle N_{\text{pairs}}(\nu)\right\rangle = \frac{1}{2}\cdot\nu\cdot\frac{\nu_{\text{coord}}\cdot(\nu-1)}{N_L-1} \tag{35}$$

Let us now treat the influx terms due to 2nd-order reaction events:

$$\sum_{x_1=1}^{N_L-\nu+1}\ \cdots\ \sum_{x_\nu=x_{\nu-1}+1}^{N_L}\ \sum_{\substack{p=1,\ldots,N_L\\ p\neq x_i\forall i=1,\ldots,\nu}}\ \sum_{\substack{q=p+1,\ldots,N_L\\ q\neq x_i\forall i=1,\ldots,\nu}} k_{\text{rxn}2}\cdot\mathbf{1}_{\{p\text{ neighbors }q\}}\cdot P_0\left(x_1,\ldots,p,\ldots,q,\ldots,x_\nu\,|\,\nu+2;t\right) \tag{36}$$

The above expression averages over all possible configurations of $\nu + 2$ adparticles: $\nu$ particles at sites $x_1,\ldots,x_\nu$ and two additional adparticles occupying sites p and q. Note though that since the site counters p and q do not appear in a sequence of ordered sums (unlike $x_1,\ldots,x_\nu$), some configurations of the $\nu + 2$ particles appear repetitively in the summed expression. To overcome this complication we introduce the indicator variable $\mathbf{1}_{\{x_i\text{ ranks }\xi\}}$ which evaluates to 1 if site $x_i$ appears in the $\xi^{\text{th}}$ position in an ordered list of sites $x_1,\ldots,x_\nu$. In our case we are concerned with the order of sites p and q in the ordered list $x_1,\ldots,p,\ldots,q,\ldots,x_\nu$. Thus we can write:

$$\begin{aligned}
&\sum_{x_1=1}^{N_L-\nu+1}\ \cdots\ \sum_{x_\nu=x_{\nu-1}+1}^{N_L}\ \sum_{\substack{p=1,\ldots,N_L\\ p\neq x_i\forall i=1,\ldots,\nu}}\ \sum_{\substack{q=p+1,\ldots,N_L\\ q\neq x_i\forall i=1,\ldots,\nu}} \bullet\ = \\
&\sum_{x_1=1}^{N_L-\nu+1}\ \cdots\ \sum_{x_\nu=x_{\nu-1}+1}^{N_L}\ \sum_{\substack{p=1,\ldots,N_L\\ p\neq x_i\forall i=1,\ldots,\nu}}\ \sum_{\substack{q=p+1,\ldots,N_L\\ q\neq x_i\forall i=1,\ldots,\nu}}\ \sum_{\zeta=1}^{\nu+1}\sum_{\xi=\zeta+1}^{\nu+2}\mathbf{1}_{\{p\text{ ranks }\zeta\}}\cdot\mathbf{1}_{\{q\text{ ranks }\xi\}}\bullet\ = \\
&\sum_{\zeta=1}^{\nu+1}\sum_{\xi=\zeta+1}^{\nu+2}\sum_{x_1=1}^{N_L-\nu+1}\ \cdots\ \sum_{x_\nu=x_{\nu-1}+1}^{N_L}\ \sum_{\substack{p=1,\ldots,N_L\\ p\neq x_i\forall i=1,\ldots,\nu}}\ \sum_{\substack{q=p+1,\ldots,N_L\\ q\neq x_i\forall i=1,\ldots,\nu}}\mathbf{1}_{\{p\text{ ranks }\zeta\}}\cdot\mathbf{1}_{\{q\text{ ranks }\xi\}}\bullet
\end{aligned} \tag{37}$$

The latter expression sums over the possible orders of p and q ($\zeta$ and $\xi$, respectively). Furthermore, for fixed $\zeta$ and $\xi$ the summations over p and q can be incorporated into the sequence of ordered sums over $x_1,\ldots,x_\nu$ and eliminate the rank indicators. Using this reasoning we conclude that:

$$\begin{aligned}&\sum_{x_1=1}^{N_L-\nu+1}\ \cdots\ \sum_{x_\nu=x_{\nu-1}+1}^{N_L}\ \sum_{\substack{p=1,\ldots,N_L\\ p\neq x_i\,\forall i=1,\ldots,\nu}}\ \sum_{\substack{q=p+1,\ldots,N_L\\ q\neq x_i\,\forall i=1,\ldots,\nu}} k_{rxn2}\cdot \mathbf{1}_{\{p\text{ neighbors }q\}}\cdot P_0\left(x_1,\ldots,p,\ldots,q,\ldots,x_\nu\,|\,\nu+2;t\right) = \\ &\sum_{\zeta=1}^{\nu+1}\sum_{\xi=\zeta+1}^{\nu+2}\sum_{x_1=1}^{N_L-\nu+1}\ \cdots\ \sum_{x_{\nu+2}=x_{\nu+1}+1}^{N_L} k_{rxn2}\cdot \mathbf{1}_{\{x_\zeta\text{ neighbors }x_\xi\}}\cdot P_0\left(x_1,\ldots,x_\zeta,\ldots,x_\xi,\ldots,x_\nu\,|\,\nu+2;t\right)\end{aligned} \tag{38}$$

Consequently, we can apply our previous reasoning and write:

$$\begin{aligned}&\sum_{x_1=1}^{N_L-\nu+1}\ \cdots\ \sum_{x_\nu=x_{\nu-1}+1}^{N_L}\ \sum_{\substack{p=1,\ldots,N_L\\ p\neq x_i\,\forall i=1,\ldots,\nu}}\ \sum_{\substack{q=p+1,\ldots,N_L\\ q\neq x_i\,\forall i=1,\ldots,\nu}} k_{rxn2}\cdot \mathbf{1}_{\{p\text{ neighbors }q\}}\cdot P_0\left(x_1,\ldots,p,\ldots,q,\ldots,x_\nu\,|\,\nu+2;t\right) = \\ &\frac{1}{2}\cdot k_{rxn2}\cdot\left\langle N^{\text{occp site}}_{\text{occp neigh,j}}(\nu+2)\right\rangle = \frac{1}{2}\cdot k_{rxn2}\cdot\frac{\nu_{coord}\cdot(\nu+2)\cdot(\nu+1)}{N_L-1}\end{aligned} \tag{39}$$

Finally, by collecting the averaged terms, we end up with a birth-death master equation for the number of adparticles:

$$\begin{aligned}\frac{\partial P_0(\nu;t)}{\partial t} = {}& k_{ads}\cdot(N_L-\nu+1)\cdot P_0(\nu-1;t) - k_{ads}\cdot(N_L-\nu)\cdot P_0(\nu;t) + \\ & k_{des}\cdot(\nu+1)\cdot P_0(\nu+1;t) - k_{des}\cdot\nu\cdot P_0(\nu;t) + \\ & k_{rxn1}\cdot(\nu+1)\cdot P_0(\nu+1;t) - k_{rxn1}\cdot\nu\cdot P_0(\nu;t) + \\ & \frac{k_{rxn2}\cdot\nu_{coord}}{2\cdot(N_L-1)}\cdot(\nu+2)\cdot(\nu+1)\cdot P_0(\nu+2;t) - \frac{k_{rxn2}\cdot\nu_{coord}}{2\cdot(N_L-1)}\cdot\nu\cdot(\nu-1)\cdot P_0(\nu;t)\end{aligned} \tag{40}$$

## 4. LATTICE STATE COORDINATE TRANSFORMATION

To illustrate the coordinate transformation from the occupancy vector $\boldsymbol{\sigma}$ to the number and positions of particles $(\nu,x_1,\ldots,x_\nu)$, we present the following example. Consider a lattice with $N_L = 3$ sites, labeled 1, 2, 3. Then there are 8 possible configurations that can be represented in terms of the occupancy vector or the adparticles' number and positions (see table on the right).

| $\boldsymbol{\sigma}$ | $(\nu,x_1,\ldots,x_\nu)$ |
|---|---|
| (0, 0, 0) | (0) |
| (1, 0, 0) | (1, 1) |
| (0, 1, 0) | (1, 2) |
| (0, 0, 1) | (1, 3) |
| (1, 1, 0) | (2, 1, 2) |
| (1, 0, 1) | (2, 1, 3) |
| (0, 1, 1) | (2, 2, 3) |
| (1, 1, 1) | (3, 1, 2, 3) |

In the occupancy vector representation, (1, 0, 1) means that sites 1 and 3 are occupied. The sets of configurations that have the same number of particles belong to discrete planes that satisfy $0 \le \sigma_1 + \sigma_2 + \sigma_3 = \nu \le N_L$ and are shown in the left plot of the following figure. The plane for $\nu = 0$

has only one point (0, 0, 0); for ν = 1, there are 3 points (1, 0, 0); (0, 1, 0); (0, 0, 1), etc.

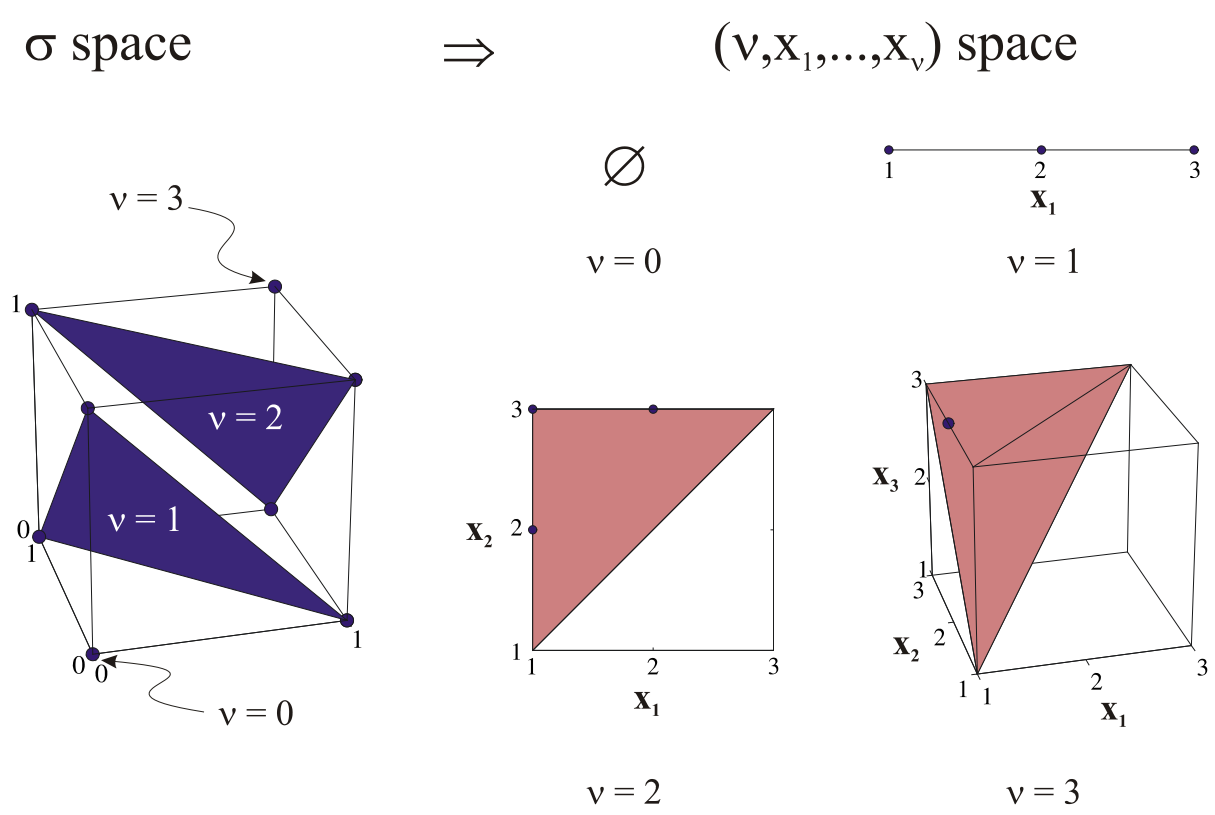


*Representation of the possible lattice configurations for a 3-site lattice in* $\boldsymbol{\sigma}$ *and* $(\nu,x_1,\ldots,x_\nu)$ *coordinates.*

In the number and positions representation, (2, 1, 3) means that there are 2 adparticles on the lattice (first element of the vector), which are found at sites 1 and 3. Thus, the sets of configurations that have the same number of adparticles belong to discrete pyramids in $\mathbb{N}^\nu$, which satisfy $1 \le x_1 < x_2 < x_3 \le N_L$, shown in the right plot of the figure.

## REFERENCES


1. Haseltine, E.L. and J.B. Rawlings, *Approximate simulation of coupled fast and slow reactions for stochastic chemical kinetics.* The Journal of Chemical Physics, 2002. **117**(15): p. 6959-6969.
2. Haseltine, E.L. and J.B. Rawlings, *On the origins of approximations for stochastic chemical kinetics.* The Journal of Chemical Physics, 2005. **123**: p. 164115.
3. Gillespie, D.T., *A general method for numerically simulating the stochastic time evolution of coupled chemical reactions.* Journal of Computational Physics, 1976. **22**(4): p. 403-434.
4. Gillespie, D.T., *Exact stochastic simulation of coupled chemical reactions.* The Journal of Physical Chemistry, 1977. **81**(25): p. 2340-2361.

5. Salis, H. and Y. Kaznessis, *Accurate hybrid stochastic simulation of a system of coupled chemical or biochemical reactions.* The Journal of Chemical Physics, 2005. **122**: p. 054103.
6. Salis, H. and Y.N. Kaznessis, *An equation-free probabilistic steady-state approximation: Dynamic application to the stochastic simulation of biochemical reaction networks.* The Journal of Chemical Physics, 2005. **123**: p. 214106.
7. Hill, A.D., et al., *SynBioSS: the synthetic biology modeling suite.* Bioinformatics, 2008. **24**(21): p. 2551-2553.
8. Salis, H., V. Sotiropoulos, and Y.N. Kaznessis, *Multiscale Hy3S: Hybrid stochastic simulation for supercomputers.* BMC Bioinformatics, 2006. **7**: p. 93.
9. Rao, C.V. and A.P. Arkin, *Stochastic chemical kinetics and the quasi-steady-state assumption: Application to the Gillespie algorithm.* The Journal of Chemical Physics, 2003. **118**(11): p. 4999-5010.
10. Cao, Y., D.T. Gillespie, and L.R. Petzold, *The slow-scale stochastic simulation algorithm.* Journal of Chemical Physics, 2005. **122**(1): p. 014116.
11. Cao, Y., D. Gillespie, and L. Petzold, *Multiscale stochastic simulation algorithm with stochastic partial equilibrium assumption for chemically reacting systems.* Journal of Computational Physics, 2005. **206**(2): p. 395-411.
12. Samant, A. and D.G. Vlachos, *Overcoming stiffness in stochastic simulation stemming from partial equilibrium: A multiscale Monte Carlo algorithm.* Journal of Chemical Physics, 2005. **123**(14): p. 144114.
13. Samant, A., B.A. Ogunnaike, and D.G. Vlachos, *A hybrid multiscale Monte Carlo algorithm (HyMSMC) to cope with disparity in time scales and species populations in intracellular networks.* BMC Bioinformatics, 2007. **8**: p. 175.
14. E, W., D. Liu, and E. Vanden-Eijnden, *Nested stochastic simulation algorithm for chemical kinetic systems with disparate rates.* Journal of Chemical Physics, 2005. **123**(19): p. 194107.
15. Weinan, E., D. Liu, and E. Vanden-Eijnden, *Nested stochastic simulation algorithms for chemical kinetic systems with multiple time scales.* Journal of Computational Physics, 2007. **221**(1): p. 158-180.
16. Peles, S., B. Munsky, and M. Khammash, *Reduction and solution of the chemical master equation using time scale separation and finite state projection.* Journal of Chemical Physics, 2006. **125**(20): p. 204104.
17. Mastny, E.A., E.L. Haseltine, and J.B. Rawlings, *Two classes of quasi-steady-state model reductions for stochastic kinetics.* Journal of Chemical Physics, 2007. **127**(9): p. 094106.
18. Mastny, E.A., E.L. Haseltine, and J.B. Rawlings, *Stochastic simulation of catalytic surface reactions in the fast diffusion limit.* Journal of Chemical Physics, 2006. **125**(19): p. 194715.